AD-A102 015 HYDROLOGIC ENGINEERING CENTER DAVIS CA F/G 8/8
GUIDELINES FOR CALCULATING AND ROUTING A DAM-BREAK FLOOD.(U)
JAN 77 D L GUNDLACH, W A THOMAS
UNCLASSIFIED HEC-RN-5 NL

1 OF 1
AD
A102015

END
DATE
FILMED
8 81
DTIC

RESEARCH NOTE NO. 5

GUIDELINES FOR CALCULATING AND ROUTING A DAM-BREAK FLOOD

JANUARY 1977

HEC

THE HYDROLOGIC ENGINEERING CENTER
- research
- training
- application

CORPS OF ENGINEERS
U. S. ARMY

UNCLASSIFIED

SECURITY CLASSIFICATION OF THIS PAGE (When Data Entered)

REPORT DOCUMENTATION PAGE		READ INSTRUCTIONS BEFORE COMPLETING FORM
1. REPORT NUMBER Research Note No. 5	2. GOVT ACCESSION NO. AD-A102	3. RECIPIENT'S CATALOG NUMBER 015
4. TITLE (and Subtitle) GUIDELINES FOR CALCULATING AND ROUTING A DAM-BREAK FLOOD		5. TYPE OF REPORT & PERIOD COVERED
		6. PERFORMING ORG. REPORT NUMBER
7. AUTHOR(s) David L. Gundlach and William A. Thomas		8. CONTRACT OR GRANT NUMBER(s)
9. PERFORMING ORGANIZATION NAME AND ADDRESS U.S. Army Corps of Engineers The Hydrologic Engineering Center 609 Second Street, Davis, CA 95616		10. PROGRAM ELEMENT, PROJECT, TASK AREA & WORK UNIT NUMBERS
11. CONTROLLING OFFICE NAME AND ADDRESS		12. REPORT DATE January 1977
		13. NUMBER OF PAGES 60
14. MONITORING AGENCY NAME & ADDRESS(if different from Controlling Office)		15. SECURITY CLASS. (of this report) Unclassified
		15a. DECLASSIFICATION/DOWNGRADING SCHEDULE

16. DISTRIBUTION STATEMENT (of this Report)

Distribution of this publication is unlimited.

17. DISTRIBUTION STATEMENT (of the abstract entered in Block 20, if different from Report)

18. SUPPLEMENTARY NOTES

19. KEY WORDS (Continue on reverse side if necessary and identify by block number)

Dam failure, Flood profiles, Model studies, Waves(Water), Open channel flow, Flood routing, Mathematical models, Analytical techniques, Analysis, Hydrographs, Hydrograph analysis, Water levels, Discharge(Water), Reservoirs, Peak discharge, Rupturing, Unsteady flow, Steady flow, Teton Dam.

20. ABSTRACT (Continue on reverse side if necessary and identify by block number)

This report described procedures necessary to calculate and route a dam-break flood using an existing generalized unsteady open channel flow model. The recent Teton Dam event was reconstituted to test the model's performance on such a highly dynamic wave. The procedures outlined relate, primarily, to partial breaches. Some deficiencies in the model were identified which will require some further (CONTINUED)

DD FORM 1 JAN 73 1473 EDITION OF 1 NOV 65 IS OBSOLETE

SECURITY CLASSIFICATION OF THIS PAGE (When Data Entered)

20 (CONTINUED)

research and programming to improve the applicability of the program to dam-break flood events. The special project memo established four objectives for this study. The first two, (1) level of accuracy of existing techniques and (2) sensitivity of calculated results to n-values and breach size, were summarized and presented in detail in Appendix A. The third objective, (3) description of physical phenomena controlling depth and travel time and a discussion of pertinent field data, was presented in the body of this report. The fourth objective, (4) documentation of the methodology, was included in Appendix B. Computer programs utilized in the methodology may be obtained from The Hydrologic Engineering Center. The computer program was applied to the Teton Dam data set to demonstrate the level of accuracy one might expect in such analyses. The results were shown and, in general, appear reasonable.

14 HEC-RN-5

RESEARCH NOTE NO. 5

GUIDELINES FOR CALCULATING AND ROUTING A DAM-BREAK FLOOD

by

DAVID L. GUNDLACH
WILLIAM A. THOMAS

January 1977

12 65

THE HYDROLOGIC ENGINEERING CENTER
CORPS OF ENGINEERS, U.S. ARMY
609 SECOND STREET
DAVIS, CALIFORNIA
95616

FOREWORD

This Research Note reports the findings of The Hydrologic Engineering Center on appropriate methodologies for calculating and routing floods resulting from suddenly-breached dams.

This study was prepared for the U.S. Army Engineer Waterways Experiment Station, Vicksburg, Miss. with funding provided by the Defense Nuclear Agency under subtask L19HAXSX337, "Above Ground Structures," work unit 07, "Damage of Dams," and by the Office, Chief of Engineers under DA project 4A762719AT40, task A1, work unit 006.

The material contained herein is offered for information purposes only and should not be construed as Corps of Engineers policy or as being recommended guidance for field offices of the Corps of Engineers.

GUIDELINES FOR

CALCULATING AND ROUTING A DAM-BREAK FLOOD

Table of Contents

LIST OF TABLES

LIST OF FIGURES

APPENDICES

APPENDIX A

Unsteady Flow Analysis - Teton Dam Failure

Table of Contents

LIST OF TABLES

LIST OF PLATES

APPENDIX B

Guidelines for Analyzing a Dam Break Flood with the Computer Program "Gradually Varied Unsteady Flow Profiles"

Table of Contents

RESEARCH NOTE NO. 5

GUIDELINES FOR CALCULATING AND ROUTING A DAM-BREAK FLOOD

1. Introduction. Planning and design requirements for a wide range of projects, such as emergency preparedness and siting of nuclear power plants, have generated widespread interest in dam break floods. Much academic research and some laboratory research have been accomplished on this topic. Generalized analytic techniques for calculating and routing such floods, particularly in non-prismatic valleys, have not been readily available. Furthermore, prototype verification data are almost non-existent. This report describes procedures necessary to calculate and route a dam break flood using an existing generalized unsteady open channel flow model. The recent Teton Dam event was reconstituted to test the model's performance on such a highly dynamic wave. The procedures outlined herein relate, primarily, to partial breaches. Some deficiencies in the model were identified which will require some further research and programming to improve the applicability of the program to dam break flood events.

2. Summary. The special projects memo cited as reference (a) established four objectives for this study. The first two, a) level of accuracy of existing techniques and b) sensitivity of calculated results to n-values and breach size, are summarized below and presented in detail in Appendix A. The third objective, c) description of physical phenomena controlling depth and travel time and a discussion of pertinent field data, is presented in the body of this report. The fourth objective, d) documentation of the methodology, is included in Appendix B. Computer programs utilized in the methodology, references (b) and (c), may be obtained from The Hydrologic Engineering Center.

The computer program of reference (c) was applied to the Teton Dam data set to demonstrate the level of accuracy one might expect in such analyses. The results are shown on pages A-26 through A-28 of Appendix A and, in general, appear reasonable. This test case demonstrates the usefulness of a generalized computer program because the methods proposed in references (d) and (e) were not applicable to the Teton data set for reasons given in paragraph 10.

Regarding sensitivity to breach size, pages A-22 and A-23 show the two breach sizes considered. The breach that developed at Teton was estimated, by others, to be 40 percent of the dam embankment. Geometric data were not available to verify this, therefore, our best estimate of the final Teton breach geometry, page A-22, is based on photographs. The breach shown on page A-23 has the same side slope as that on page A-22, 0.6 on 1, but it has zero bottom width. This seemed a likely intermediate condition, but no field data were available at the time of this study to establish an observed intermediate condition.

The calculated outflow is shown on page A-24. The hydrograph labeled "trapezoidal breach" assumed the 40 percent breach size, page A-22, developed instantaneously. The hydrograph labeled "triangular breach" was determined in a similar manner for the 30% breach size. The third hydrograph on page A-24 was calculated for the trapezoidal breach (labeled 40% breach size on page A-22), but an observed reservoir drawdown curve at the dam, page A-20, was used which implies a gradual development of the breach rather than instantaneous failure. The last approach was considered best in estimating the discharge hydrographfrom Teton reservoir given the data set and analytical techniques available to us.

The sensitivity of calculated outflows to breach size and rate of development is illustrated on page A-24. It is summarized in the following table together with pertinent elevation data for an n value of 0.04.

Table 1: Sensitivity to Breach Size and Rate of Development

Final Breach Size % of Total Dam	Rate of Development	Calculated Peak Water Discharge at Dam Axis 10^6 CFS (1)	Calculated Peak Elevations MSL		
			At Dam Axis	Miles Downstream from Dam Axis	
				5	10
40%	(2)	1.8 (3)	5123	5014	4933
30%	instantaneous	2.4	5151	5015	4933
40%	instantaneous	3.4	5175	5020	4935

(1) Multiply by 0.02832 to get Cubic Meters Per Second

(2) Actual rate of development was unknown so the observed reservoir drawdown curve, page A-20, was used to approximate outflow conditions.

(3) The actual peak discharge, as estimated by personnel of the Walla Walla District, Army Corps of Engineers from observed data in the Teton Canyon three miles downstream from the dam, was 2,300,000 cfs.

From these results it is apparent that neither the size of breachs tested nor the rates of failure assumed were very significant in predicting peak elevations five miles downstream from the dam.

The calculated peak flood elevations, near the dam, were very sensitive to n-values. Increasing n from .03 to .06 raised the peak flood elevation 25 feet at the dam, as illustrated on page A-8, Table 3. At 5 miles downstream the calculated difference was only 8 feet. Differences continued to diminish with distance.

Calculated Travel Times are shown on page A-29. They correspond to the discharge hydrograph labeled "simulated from observed data" on page A-24 and n-values of 0.04.

Searching for a simplified approach in place of references (d) and (e) led to a trial application of the Modified Puls routing technique. The hydrograph labeled "simulated from observed data" on page A-24 was routed and a water surface profile calculated for the resulting peak discharges. A comparison of the results with the observed elevations and the peak elevations computed with the full equations is shown on pages A-30 through A-32. Additional investigation is needed to establish the range of applicability of this method.

3. Physical Phenomena and Field Data. Analysis of the dam-break flood involves understanding the physical processes before applying analytical techniques which approximate those physical processes. Three distinctly different processes are involved: the process of structural failure causing the breach to develop; the process of setting water into motion in a reservoir; and the process of flood wave attenuation.

The size, shape and rate of breach development are primarily responsible for the peak rate of outflow from the reservoir. Yet, of the three physical processes, this one is the most difficult to quantify. With the exception of man-made breaches, it is difficult to visualize the instantaneous development of a breach. Some have occurred, however. The St. Frances Dam, a high head concrete gravity structure, apparently suffered an abutment failure which resulted in virtually the instantaneous failure of the entire structure. The Johnstown flood of 1889 was caused by the complete failure of an earth fill dam. Reports indicate that less than half an hour was required for overtopping flow to breach the structure. The recent Teton failure, a full depth-partial width breach of an earth fill dam, is estimated to have developed in less than two hours. Since natural failure of a major structure is so improbable, establishing a mode of failure requires a policy decision rather than an analytical technique. In general, instantaneous failure of the entire structure produces the largest flood wave.

The second physical process results from the depth of water above the breach invert. That is, a reservoir has a total energy head equal to the elevation of the water surface. If the dam is breached, the force of gravity will set water into motion. The effect will propogate, as a negative wave, to the upstream end of the reservoir at a velocity equal to $\sqrt{gy}$ where g is acceleration of gravity and y is water depth. Because of the great depth in a reservoir, very little frictional resistance is mobilized during the passage of this negative wave. As a result, water gains specific energy rapidly as it moves toward the breach. In instantaneous breach development, the peak outflow will occur within a minute or two after breaching.

Whereas the total energy head setting the water into motion is the specific energy (i.e., the initial water depth) above the breach invert, the energy which must be dissipated in the downstream channel is equal to the specific energy from the downstream channel invert to the initial pool elevation. The fact that the water surface elevation drops down rapidly at the dam axis does not reflect a corresponding loss in energy head. When flow begins, that specific energy above the breach invert is transformed into three components: a pressure head, a kinetic energy head and an inertia head. (The relative size of each of these energy head components is discussed more fully in sections 4 and 5.) Friction loss is relatively small and may be neglected unless the reservoir bottom is extremely rough (more than 5% or 10% of the water depth).

The third physical process, flood wave attenuation, involves energy dissipation and valley storage. As the flood wave moves downstream, the peak discharge tends to decrease, the base of the flood wave will become longer and the wave velocity will decrease. Near the dam, energy dissipation is primarily responsible for behavior of the flood wave. However, valley storage soon becomes the primary factor in flood wave attenuation. The key to the transition from energy dissipation to valley storage control is the rate at which the slope of the total energy gradient, a line which must intersect the initial pool elevation at the dam, is reduced to that of a major rainfall flood in the downstream valley. It seems obvious that the total energy at any cross section in the valley should not exceed the initial reservoir elevation, and yet some analytical techniques occasionally violate that constraint. It is good policy to always check the total energy, as well as the water volume, in a calculated flood wave.

The rate of energy dissipation is governed primarily by friction loss. Minor losses from bends and contractions-expansions are often included in the n-values.

The volume of water in the reservoir is the final piece of field data required. This volume strongly influences the peak elevations at downstream points.

4. <u>Energy Components and Peak Outflow from Complete, Instantaneous Breaches.</u> It is useful to develop the relative size for each energy component in the flow at the dam axis and to compare all of them to the more common case of steady state critical flow at a contraction.

By assuming a rectangular cross section, zero bottom slope and instantaneous removal of the entire dam, Saint-Venant developed an analytical solution for the elevation of the free surface, reference (f). page 755. Utilizing that equation, the depth of flow at the dam axis was determined, by Saint-Venant and others, to be $\frac{4}{9} Y_0$ where Y_0 is the original water depth at the dam. Also, the velocity corresponding to the peak outflow was shown to be $\frac{2}{3}\sqrt{gY_0}$. Combining these relationships leads to the equation for peak discharge

$$q_{max} = \frac{8}{27} Y_0 \cdot \sqrt{g \cdot Y_0} \qquad (1)$$

Y_0 is the initial water depth at the dam

g is acceleration of gravity

q_{max} is peak water discharge in cfs/ft

Since this equation was developed for a rectangular section, the total *discharge may be calculated by multiplying* q_{max} by the width.

Using the relationships referenced above, the velocity head (i.e., the kinetic energy head component of the specific energy head) was calculated to be $\frac{2}{9} Y_0$. Since, in the absence of friction and other losses, inertia is the only remaining term in the basic, unsteady flow equations of Saint-Venant, it may be calculated as follows.

$$Y_0 = h_i + \frac{2}{9} Y_0 + \frac{4}{9} Y_0 \qquad (2)$$

$$h_i = \frac{3}{9} Y_0$$

These components are shown in Figure 1 along with the energy components for critical, steady state flow.

This figure shows that in the dam break flood analysis, as well as steady state critical flow at a contraction, the velocity head is half the pressure head. However, the inertia head component is zero in Figure 1a because flow is steady state.

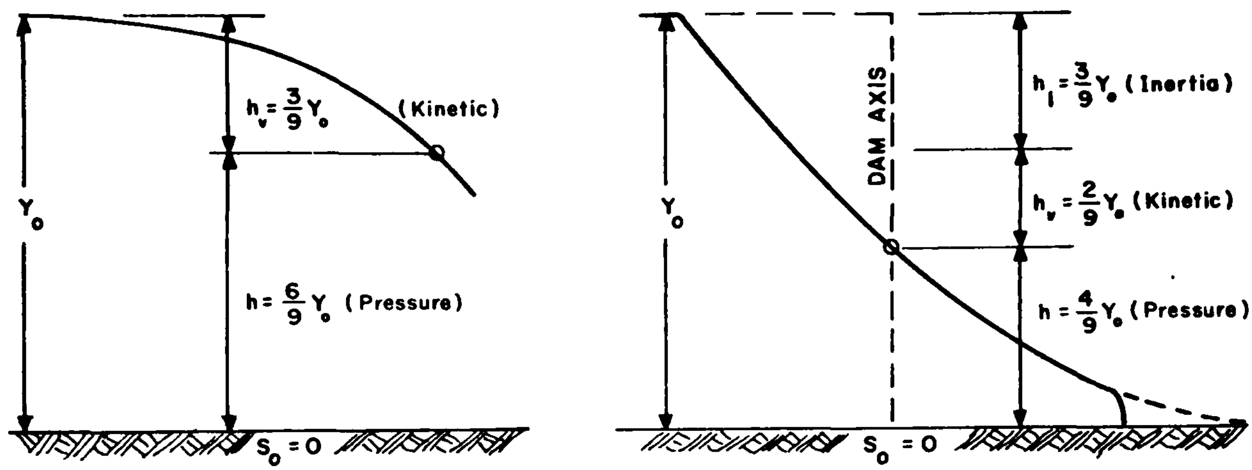

(a) Critical flow at a contraction (steady flow conditions)

(b) Critical flow from a breached dam (unsteady flow conditions)

Figure 1. Components of Specific Energy Head.

The drawdown in water surface elevation to $\frac{4}{9} Y_0$ at the dam axis, Figure 1b, does not reflect a corresponding energy loss. Experimental results obtained by Schoklitsch, reproduced on page 755 of reference 1f, show relatively little friction loss in flow approaching the dam axis. As might be expected, the model results showed friction to be very significant downstream. Tests reported by WES in reference (g) showed no impact from friction loss at the dam axis. However, the WES flume sloped at 0.005 ft/ft, whereas the flume in Schoklitsch's experiment had zero bottom slope.

The significance of this point is that all three energy components, pressure head, kinetic energy head and inertia head, are significant in complete, instantaneous breachings. Consequently, investigators encourage the use of the complete routing equations, often referred to as the Saint-Venant equations. Simplifications of the complete equations, such as Muskingham, Tatum, Straddle-Stagger and Modified Puls, are not recommended because the empirical coefficients would invariably be developed from rainfall floods and would reflect different values of energy components relative to Y_0.

5. Instantaneous, Partial Breaches. Partial breaches are classified, according to hydraulic performance, as full depth-partial width, partial depth-full width or partial depth-partial width. A separate equation has been developed for calculating the peak water discharge for each class, page 25 of reference (g).

Full Depth-Partial Width

$$Q_{max} = \frac{8}{27} \cdot b \cdot Y_o \cdot \left(\frac{B}{b}\right)^{\frac{1}{4}} \sqrt{gY_o} \qquad (3)$$

B is width of channel, feet
b is width of breach, feet

Partial Depth-Full Width

$$Q_{max} = \frac{8}{27} \cdot B \cdot y\left(\frac{Y_o}{y}\right)^{\frac{1}{3}} \sqrt{gy} \qquad (4)$$

y is depth of water above bottom of breach

Partial Depth-Partial Width

$$Q_{max} = \frac{8}{27} \cdot b \cdot y \cdot \left(\frac{B}{b}\right)^{\frac{1}{4}} \cdot \left(\frac{Y_o}{y}\right)^{\frac{1}{3}} \sqrt{gy} \qquad (5)$$

An empirical equation for partial depth-partial width breaches was reported in references (g) and (h).

$$Q_{max} = 0.29 \cdot b \cdot y \cdot \left(\frac{B}{b} \cdot \frac{Y_o}{y}\right)^{0.28} \cdot \sqrt{gy} \qquad (6)$$

For breach sizes in the following range.

$$1 \leq \left(\frac{B}{b} \cdot \frac{Y_o}{y}\right) \leq 20 \qquad (7)$$

Since the discharge equations for partial breaches are similar, in form, to that for a full breach (1), the total specific energy has the same three basic components. However, their size, relative to initial water depth, is considerably different from that shown in Figure 1. There is no analytical solution for partial breaches, therefore, experimental results, presented in reference(g), were used to calculate the individual energy head components. The following table presents experimental results for full depth breaches ranging in width from 10% to 100% of the flume width in columns 1, 2 and 3. Fractions of initial water depth, calculated with equation 3, are shown in columns 4 and 5. A sample of the calculations is presented in the paragraph following the table. This sample calculation utilizes equation 3 and a 100% breach size (i.e., full breach) to demonstrate that the relative value of each energy component is the same as the respective value produced by equation 1, the analytical, full breach equation, when equation 3 is carried to its upper limit.

Table 2: Relative Size of Energy Components in Partial Width Breaches[1]

Test No	Breach Size %	Pressure Head % of Y_o	Velocity Head (2) % of Y_o	Inertia Head (3) % of Y_o
(1)	(2)	(3)	(4)	(5)
1.1	Full	44	22	34
2.1	60	70	12	18
3.1	30	82	12	6
4.1	15	89	(4)	- -
5.1	10	94	(4)	- -

Notes: 1. Values in columns 1 and 2 are from Table 4, page 8, reference (g) and values in column 3 are from experimental results from Tables 1 through 5, Station 200, reference (g).

2. Velocity head is calculated with equations 8 and 9, following.

3. Inertia head is Y_o - (pressure head + velocity head).

4. Calculated values exceeded 100 percent of Y_o, which probably reflects scatter in experimental results.

$$V_{max} = \frac{Q_{max}}{b \cdot y} \tag{8}$$

where:

y = depth of water at dam axis

b = breach width

Q_{max} from equation (3)

$$V_{max} = \frac{\frac{8}{27} \cdot b \cdot Y_o \left(\frac{B}{b}\right)^{\frac{1}{4}} \sqrt{gY_o}}{b \cdot y} \tag{9}$$

For the full breach, $b = 1.0B$ and $y = \frac{4}{9} Y_o$

$$V_{max} = \frac{\frac{8}{27} \cdot Y_o \left(\frac{B}{1.0B}\right)^{\frac{1}{4}} \sqrt{gY_o}}{\frac{4}{9} \cdot Y_o} \tag{10}$$

$$V_{max} = \frac{2}{3} \sqrt{gY_o} \tag{11}$$

$$\frac{V^2_{max}}{2g} = \frac{4}{9} \frac{gY_o}{2g} \tag{12}$$

$$= \frac{2}{9} Y_o \tag{13}$$

This agrees with section 4 and shows the procedure followed in completing Table 2. The inertia head, column 5 in Table 2, was calculated assuming zero energy loss upstream from the dam.

$$Y_o = h_i + \frac{2}{9} Y_o + \frac{4}{9} Y_o \tag{14}$$

$$h_i = \frac{3}{9} Y_o \tag{15}$$

Because of the decrease in relative significance of inertia head and even velocity head, it is satisfactory to apply simplifications of the full Saint-Venant equations to partially breached dams.

6. Attenuation of the Flood Wave. As a flood wave moves downstream, friction and other losses change the relative size of the three energy components. Even floods from fully breached dams eventually take on the characteristics of a rainfall flood and may be routed with a simplified routing method such as Modified Puls. Major areas of uncertainty are 1) how much distance is required for this transition, 2) how does this distance vary when considering partial breaches and 3) what is the maximum breach size to consider as a partial breach.

7. Proposed Analytical Technique. The guidelines presented in Appendix B of this report are developed for the computer program "Gradually Varied Unsteady Flow Profiles". It is a solution of the basic Saint-Venant equations for unsteady flow and may be used to calculate the outflow hydrograph through any size or shape of breach, as well as to route that hydrograph downstream and provide water discharge and water surface elevation

hydrographs at any number of computation points up to 45. The maximum discharge, maximum elevation and maximum flow velocity are summarized for each computation point.

Sufficient information is printed out so the time of arrival, time of peak and duration of the flood may be plotted.

This computer program accounts for the movement of the negative wave through the reservoir, for the tailwater submergence at the dam, for the three components of energy presented earlier, for friction loss and for storage in the reservoir and the downstream valley.

Cross sections need not be rectangular or prismatic. A companion program, "Geometric Elements from Cross Section Coordinates", is available to transform complex cross sections into the required geometric data set for the routing program.

These computer programs are generalized. That is, they are sufficiently flexible and adaptable to be used without code changes. They are portable from one computer to another and documentation is available, from The Hydrologic Engineering Center.

8. Program Limitations.

a. Routing with the Gradually Varied Unsteady Flow Profiles computer program requires a large high speed computer (50,000, 60-bit words) and personnel who are experienced in applying mathematical models.

b. Any breach size may be modeled, but the program assumes instantaneous development.

c. All channels must be wet initially. That is, computations cannot be made if any portion of the model is dry. This is overcome by prescribing a base flow; however, the computer program has difficulty in establishing this profile.

d. Movement of the negative wave through the reservoir causes no computational problem until it reaches the upstream end of the reservoir. Computation nodes tend to go dry and abort the computer run.

e. The analysis of multiple failures would require manual intervention to stop and restart the calculation process as each new structure is brought into the system.

f. The program assumes a horizontal water surface transverse to the flow, whereas a great deal of transverse slope can exist in the actual prototype situation.

9. Proposed Areas of Research. All of the program limitations were circumvented in analyzing the Teton Data Set. The trade-off, however, was analysis time. Seven weeks were required to set up the data, debug it and perform the analysis. The two tasks requiring the most time, probably 75%, were establishing initial base flow conditions for the model (8c) and stabilizing the computations when the negative surge reached the upstream boundary (8d). Both of these problem areas can be overcome by additional programming. The improvements would reduce analysis time to **four or five weeks.**

Instantaneous breach development, 8b, could be replaced by equations which let progressive development take place. In the absence of a theory, the rate of development would have to be prescribed with input data.

Developing the capability to handle multiple dam failures (8e), especially in tandem, will be a major modification.

This analytical technique is a one-dimensional model and will always have a horizontal water surface transverse to the flow. At present, two-dimensional modeling is not feasible.

10. Alternate Analytical Procedures. Alternate analytical procedures were proposed in references (d) and (e). Neither were applicable to the Teton Data Set.

The dimensionless curves were developed from numerical solution of the St. Venant equations and include special treatment of the wave front as it moves along a dry channel. By knowing reservoir volume, valley cross section at the dam, initial reservoir elevation, stream slope and stream roughness, the curves will provide three properties of the flood wave:

1. Time of arrival at downstream points
2. Maximum depth profile in the downstream channel
3. Time of maximum depth at downstream points.

The curves extend for distances ranging up to fifteen times the reservoir length. The outflow hydrograph at the dam is not needed to use these curves. It was assumed, in developing the curves, that the entire dam is breached instantaneously and that the valley is prismatic. Neither condition was satisfied by the Teton case.

The procedure in reference (e) was developed for smaller structures and the Teton Data Set was completely beyond the range of nomographs and curves presented there. In any case, the procedure does not route the flood wave downstream. Only the outflow discharge hydrograph is calculated at the dam axis. The procedure can handle a wide range of breach sizes, but it

is designed with partial breaches in mind. It has the advantage of tail water correction, which is essential when breaching of a low dam coincides with a high flow condition in the stream. The procedure is well documented and is easily applied.

A possible alternative approach for partial breaches is the Modified Puls routing technique. Preliminary work with this technique produced the results shown on pages A-30 through A-32 for the Teton Data Set. A Manning n value of 0.04 was used; further details are given in Paragraph 5, Appendix A. The advantage of this technique is that readily available and easily applied computer programs (e.g., HEC-1 and HEC-2) can be utilized; total analysis time would probably be reduced to two to three weeks.

The disadvantage is that the range of application is limited whereas the technique presented in Paragraph 7 is generally applicable.

Additional research is needed to define the range of applicability of the Modified Puls technique. The present hypothesis is that the size of the inertia component, Table 2, would provide a suitable parameter for defining that range.

This research would not require additional physical modeling. Studies reported in references (g) and (h) offer test data for numerical studies. Other numerical experiments could be performed by using results from analyzing variations of the Teton Data Set with the complete equations. These results could be obtained while pursuing any of the areas of research proposed in Section 9.

Computer programs which utilize the Modified Puls routing technique are available and are presently developed to a higher degree of serviceability than programs solving the full equations. Water surface profile computations will be required in conjunction with the Modified Puls routing to produce a water surface profile. These computations are computerized also. No major computer program development would be required. The appropriate existing computer programs, HEC-1 and HEC-2, are well documented.

11. References.

a. Special Projects Memo No. 473 subject Calculating and Routing the Flood Resulting from a Suddenly Breached Dam, dated 26 August 1976.

b. "Geometric Elements from Cross Section Coordinates", The Hydrologic Engineering Center, June 1976.

c. "Gradually Varied Unsteady Flow Profiles", The Hydrologic Engineering Center, June 1976.

d. "Dimensionless Graphs for Routing Floods from Ruptured Dams", by John Sakkas, dated January 1976, The Hydrologic Engineering Center.

e. "Computation of Outflow from Breached Dams", Defense Intelligence Agency, June 1963.

f. Keulegan, G.H., "Wave Motion", Engineering Hydraulics, Ed. by H. Rouse, John Wiley & Sons, Inc., New York, New York, Fifth Printing, October 1965.

g. "Flood Resulting From Suddenly Breached Dams", Conditions of Minimum Resistance, Hydraulic Model Investigation, Miscellaneous Paper No. 2-374, Report 1, U.S. Army Corps of Engineers, Waterways Experiment Station, Vicksburg, Mississippi, February 1960.

h. "Floods Resulting From Suddenly Breached Dams", Conditions of High Resistance, Hydraulic Model Investigation, Miscellaneous Paper No. 2-374, Report 2, U.S. Army Corps of Engineers, Waterways Experiment Station, Vicksburg, Mississippi, November 1961.

APPENDIX A

UNSTEADY FLOW ANALYSIS
TETON DAM FAILURE

1. INTRODUCTION

This phase of the study which calculates and routes the flood resulting from a suddenly breached dam, consists of a computer solution in conjunction with the Teton Dam failure as defined in objectives a and b of Special Projects Memo No. 473. The analysis utilizes the unsteady flow computer program to determine water surface elevations resulting from various breach sizes and n values. The level of accuracy was determined by comparing available flood data (particularly high water marks) from the June 5, 1976 dam failure with calculated results.

The analysis used data generally available to field personnel engaged in the study of the impact of a dam break flood such as topographic maps, aerial photography, dam description, gaged stream flows and reservoir elevation-capacity curves. The primary area of study included about 30 miles of flood plain downstream of the dam.

2. GENERAL DESCRIPTION

The Teton Dam is located on the Teton River in southeastern Idaho approximately 13 miles north and east of the city of Rexburg (see Plate 1). The dam was designed as a zoned earthfill embankment with a crest elevation of 5,332 feet (mean sea level datum) and a maximum height of 305 feet (above riverbed). It would create a reservoir of 288,250 acre-feet when filled to an elevation of 5,320 feet. (Plan and sections of the dam are shown in Plates 2 and 3.) The dam is located in a narrow steepwalled canyon. The channel geometry is essentially the same for some 4 miles downstream of the dam whereupon the Teton River enters upon a wide relatively flat flood plain.

The total reservoir storage just prior to failure on June 5 was about 251,300 acre-feet at an elevation of 5,301.5 feet. Measured inflow was 3,580 cubic feet per second and measured outflow before any leaks developed was 940 cubic feet per second.

Although water stored upstream of the dam caused the flooding, other sources contributed significantly to the floodflow in the downstream reaches. However, the complexity of major irrigation diversions and numerous return flows precludes an accurate accounting of all sources. According to the record obtained from the damaged recorder at the gaging station on Henrys Fork near Rexburg (at Idaho State Highway 88), 3,460 cubic feet per second

were flowing in Henrys Fork at the time the leading edge of the flood wave arrived about 4:00 p.m. on June 5. The contribution of the Snake River, just upstream of its confluence with Henrys Fork was estimated at 5,600 cubic feet per second around 1:00 p.m. of the same day.

Table 1 presents a preliminary tabulation of available data pertaining to the leading edge of the flood wave generated by the dam failure. Distances shown are measured from the dam breach along the estimated path of the leading edge of the wave.

Instantaneous peak discharges were determined at two sites along the study reach (Table 2). Indirect measurements based on field surveys and empirical formulas were used to compute the peak discharges at the sites. The indirect methods for computing peak discharge were based on hydraulic equations relating discharge to the water-surface profile and the geometry of the channel.

3. GEOMETRIC MODELS

The channel configuration upstream and downstream of the dam was modeled independently according to procedures contained in the users manual, generalized computer program (723-G2-L745B), Geometric Elements from Cross Section Coordinates (GEDA), Hydrologic Engineering Center, U.S. Army Corps of Engineers, June 1976.

The upstream geometric model (reservoir) was developed essentially from two cross sections located at the damsite and at the estimated upstream limit of the reservoir (when filled to capacity). The cross section data at the damsite were obtained for preproject conditions from topographic information shown on Plates 2 and 3. Information for the other section was obtained from U.S. Geological Survey topographic maps (scale 1:24,000). Data were coded in the standard HEC-2[1] format and input into the GEDA program. Computed results were compared with respective values taken from the reservoir capacity curve of Plate 2 and, where necessary, adjustments made to the upstream cross section until computed volumes (at specified elevations) plotted reasonably close to the published curve (see Plate 4).

The downstream model (channel) was developed in a similar manner although a more detailed definition of the channel configuration was necessary. Since the actual flooded area resulting from the dam failure included several major tributaries (the Snake River, Henrys Fork and the Teton River), there was no readily available information on storage (volume) within the study reach with which to calibrate the geometric model. Cross sections were taken on the average every mile, and conveyance limits were designated so as to effectively model conveyance for the large flows expected in the dam break analysis.

---

[1]HEC-2 Water Surface Profiles, Generalized Computer Program (723-02A), Hydrologic Engineering Center, U.S. Army Corps of Engineers, October 1973.

TABLE 1

ESTIMATED TIMES
FOR LEADING EDGE OF FLOOD WAVE
(BASED ON FIELD OBSERVATIONS)

Location	Miles[a] downstream from dam	Date (month/day)	Arrival time (hours)	Elapsed time between sites (minutes)	Approximate mean velocity between sites (ft/min)	(mi/hr)
At damsite	0.0	6-5	1157	—	—	—
In Teton Canyon	3.0	6-5	1205	8	1,980	23
At Teton	8.8	6-5	1230	25	1,220	14
At Sugar City	12.3	6-5	1300	30	620	7
At Rexburg[b]	15.3	6-5	1340	40	400	5
Henrys Fork near U.S.G.S. gaging station, Henrys Fork near Rexburg	22.6	6-5	1530	110	350	4
Menan Bridge on the Snake River immediately upstream of the Union Pacific	30.6	6-5	1800	150	280	3

[a]Distances measured along the estimated path of the leading edge of the flood wave.

[b]Maximum depths estimated at 6-8 feet within the city of Rexburg.

TABLE 2

ESTIMATED PEAK DISCHARGES
(BASED ON FIELD OBSERVATIONS)

Location	Miles[a] downstream from dam	Date (month/day)	Time (hours)	Discharge (cubic feet per second)
In Teton Canyon	3.0	6-5	b	2,300,000
At Teton	8.8	6-5	c	1,060,000

[a]Distances measured along the estimated path of the leading edge of the flood wave.

[b]Peak probably occurred between 1230 and 1330 hours.

[c]Peak probably occurred between 1300 and 1400 hours.

The area, hydraulic radius, top width and average n value were calculated at each cross section in the goemetric models for the elevations specified. By calculating length-weighted values, the preceding elements were modified such that they would apply to uniformly spaced computation points along the length of each model (reservoir and channel).

4. UNSTEADY FLOW MODELS

The unsteady flow data models of the reservoir and the channel were developed according to procedures contained in the users manual, generalized computer program (723-G2-L2450), Gradually Varied Unsteady Flow Profiles, Hydrologic Engineering Center, U.S. Army Corps of Engineers, January 1976.

Reservoir Model

In the case of the reservoir, tables of geometric elements were prepared at 21 uniformly spaced computation points (approximately 2,800 feet apart) and input into the unsteady flow program. Since inflow into the reservoir just prior to failure was measured (approximately 3,600 cubic feet per second), the upstream boundary condition was based on such. A normal depth was determined for the measured discharge rate at the upstream cross section. A steady flow condition was assumed, and a constant elevation (determined from the normal depth calculation) was specified as the boundary condition. Initial values (discharge and elevation) were specified only at the most upstream and most downstream computation points (nodes) and a linear interpolation scheme within the program utilized to determine values at the remaining nodes. The values of discharge and elevation at the upstream node are the same as those utilized in the computation of the elevation hydrograph at the upstream boundary. The elevation used at the downstream node (damsite) was 5,301.5 feet (the observed reservoir water surface elevation at time of failure) and the discharge was estimated as 3,000 cubic feet per second. (Although the measured discharge was 940 cubic feet per second before any leaks occurred, a higher discharge rate was used because of significant seepage just prior to failure). In the reconstruction of the actual discharge hydrograph at the damsite, the observed reservoir water surface elevations at particular points in time (after failure) were input initially for the downstream boundary condition (see Plate 5 for a plot of the observed data). Since the observed data were not adequate with respect to time to define a reasonable elevation hydrograph, a greater number of coordinate points were coded in the final analysis (refer to Plate 5). The computed discharge hydrograph at the damsite, based on the preceding conditions, is shown in Plate 6. (Note that the computed maximum discharge is about 1,800,000 cubic feet per second at about 2:00 p.m. of June 5.

When analyzing various breach sizes (partial failures), an elevation versus discharge curve was developed for the downstream boundary condition

(at the damsite). For the breach sizes shown in Plates 7 and 8 the discharge corresponding to various critical depths was calculated according to[1]

$$Q = \sqrt{g \frac{(b + z\,D_c)^3}{(b + 2z\,D_c)}}\; D_c^{3/2}$$

where

- b = bottom width (in feet)
- z = slope of the sides, horizontal divided by vertical
- D_c = depth (in feet)
- g = acceleration due to gravity (in feet per second per second)
- Q = discharge rate (in cubic feet per second)

After converting the various depths to elevations, the discharge rating curve corresponding to each breach size was input into the unsteady flow program. The computed discharge hydrographs are shown in Plate 9 and compared with the simulated hydrograph for observed conditions.

Preliminary information received indicated that 40 percent of the dam embankment was lost such that an initial estimate of the breach configuration (based on available photographs) is shown in Plate 7. The resulting discharge hydrograph, Plate 9, represents an instantaneous failure of the size depicted. (The same is true in the case of the triangular breach shown in Plate 8.) In the case of the discharge hydrograph computed for observed conditions, the downstream boundary condition corresponds to a gradual failure and results in significant differences in peak and in the time to peak.

In the unsteady flow analysis of the reservoir system, only the results for n values of 0.04 are included. When n values were varied, there was no significant difference in the computed discharge hydrographs at the damsite.

Channel Model

In the case of the channel, tables of geometric elements were prepared at 37 uniformly spaced computation points along the study reach (approximately 4,500 feet apart) and input into the unsteady flow program. The

---

[1] Handbook of Hydraulics, King and Brater, Fifth Ed., McGraw-Hill Book Co., 1963, pp. 8-11.

upstream boundary conditions (at the damsite) are the various discharge hydrographs computed in the unsteady flow analysis of the reservoir. The downstream boundary conditions are discharge rating curves based on normal depth calculations. The depth and corresponding discharge was determined using Manning's equation

$$Q = \frac{1.49}{n} A R^{2/3} S^{1/2}$$

where

n = coefficient of roughness

A = area (in square feet)

R = hydraulic radius (in feet)

S = slope (in feet per foot)

The values for the geometric elements, A and $R^{2/3}$, for specified depths (elevations), were taken from GEDA output for the most downstream channel cross section. The slope was determined from available topographic maps. Values of n ranged from 0.03 to 0.07, and for each n value a discharge rating curve was developed as a downstream boundary condition.

In order to simulate the actual flow existing in the probable flooded area downstream of the dam, the local inflow option of the unsteady flow program was utilized. Major inflow occurred where Henrys Fork and the Snake River entered the system. The estimated flows just prior to failure were 3,500 and 5,600 cubic feet per second respectively.

In order to establish stable base flow conditions for each n value prescribed, the model was run for a period of 24 hours with the estimated inflows at the upstream boundary and local inflow points which existed just prior to failure. (The discharge and initial approximations of water surface elevation at each node or computation point were input prior to running. Since the discharge just prior to failure was estimated from observed conditions within the study reach, values were fixed, whereas initial water surface elevations were manipulated until stable conditions resulted.) Once stable base flow conditions were obtained, the various boundary conditions (upstream and downstream) were input into the model. The model was then allowed to run until the peak of the flood hydrograph passed the downstream limit of study.

Results of the various runs are tabulated in Tables 3, 4, 5 and 6. Plate 10 is a Xerox reduction of the flooded area resulting from the June 5 dam failure as published by the U.S. Geological Survey. The relative

TABLE 3

RESULTS OF UNSTEADY FLOW ANALYSIS

USING SIMULATED DISCHARGE HYDROGRAPH

FOR OBSERVED CONDITIONS

Node No.	Maximum Elevation (feet above mean sea level)					Time of Maximum Elevation (hours - minutes)				
	n-values					n-values				
	0.03	0.04	0.05	0.06	0.07	0.03	0.04	0.05	0.06	0.07
1	5113.8	5123.4	5132.3	5138.6	5144.5	13-50	14-00	14-00	14-00	14-00
3	5091.4	5098.3	5104.8	5110.6	5115.9	14-00	14-00	14-00	14-00	14-00
5	5041.0	5046.9	5053.1	5056.5	5059.9	14-00	14-00	14-10	14-10	14-10
7	5010.0	5012.3	5014.7	5017.8	5019.9	14-10	14-20	14-20	14-20	14-20
9	4969.2	4972.0	4973.4	4974.5	4975.2	14-10	14-20	14-30	14-40	14-50
11	4948.4	4949.9	4951.2	4953.1	4954.7	14-30	14-40	14-40	14-40	14-50
13	4928.6	4929.9	4931.3	4932.3	4933.3	14-50	14-40	14-50	15-10	15-20
15	4909.0	4910.7	4911.4	4912.4	4912.9	14-40	15-00	15-20	15-30	15-50
17	4887.7	4889.1	4889.6	4890.1	4890.6	15-10	15-30	15-50	16-20	16-40
19	4865.8	4866.9	4867.5	4868.0	4868.3	15-40	16-10	16-40	17-10	17.40
21	4848.0	4848.9	4849.5	4850.1	4850.4	16-10	16-50	17-20	18-00	18-40
23	4838.0	4838.7	4839.2	4839.7	4840.0	16-40	17-30	18-20	19-00	19-50
25	4831.3	4831.8	4832.3	4832.7	4833.0	17-30	18-20	19-10	20-10	21-10
27	4824.1	4824.7	4825.3	4825.7	4826.1	18-50	20-20	21-40	22-50	24-00
29	4822.9	4823.4	4823.9	4824.4	4824.7	19-20	20-50	22-10	23-20	0-20[a]
31	4819.0	4819.7	4820.2	4820.7	4821.0	19-30	21-10	22-40	0-10[a]	1-50
33	4805.8	4806.4	4806.9	4807.3	4807.7	19-50	21-30	23-10	0-40	1-50
35	4791.4	4791.9	4792.2	4792.6	4792.8	19-40	21-30	23-10	0-40	2-10
37	4784.2	4784.7	4785.2	4785.6	4785.9	20-00	21-50	23-40	1-20	2-50

[a]June 6, 1976

TABLE 3 (*continued*)

RESULTS OF UNSTEADY FLOW ANALYSIS

USING SIMULATED DISCHARGE HYDROGRAPH

FOR OBSERVED CONDITIONS

Node No.	Maximum Discharge (cubic feet per second X 10^3)					Time of Maximum Discharge (hours - minutes)				
	n-values					n-values				
	0.03	0.04	0.05	0.06	0.07	0.03	0.04	0.05	0.06	0.07
1	1,791	1,791	1,791	1,791	1,791	14-00	14-00	14-00	14-00	14-00
3	1,811	1,808	1,792	1,776	1,758	14-00	14-00	14-00	14-00	14-00
5	1,873	1,831	1,780	1,724	1,691	14-00	14-00	14-10	14-10	14-10
7	1,987	1,766	1,713	1,757	1,740	14-10	14-20	14-10	14-20	14-20
9	1,841	1,988	1,892	1,759	1,615	14-10	14-20	14-30	14-40	14-40
11	1,876	1,768	1,796	1,919	1,939	14-20	14-40	14-30	14-40	14-50
13	1,921	1,853	1,937	1,861	1,746	14-50	14-40	14-50	15-00	15-10
15	2,257	2,184	2,082	1,972	1,796	14-40	15-00	15-10	15-30	15-40
17	2,189	2,127	1,919	1,731	1,573	15-00	15-30	15-50	16-10	16-30
19	1,812	1,585	1,400	1,255	1,122	15-40	16-10	16-30	17-00	17-30
21	1,389	1,213	1,029	919	813	16-00	16-40	17-20	17-50	18-30
23	1,039	863	751	655	589	16-30	17-20	18-00	18-40	19-30
25	708	593	525	474	434	17-20	18-00	18-50	19-40	20-30
27	676	561	489	436	396	17-30	18-30	19-20	20-20	21-20
29	521	426	369	329	301	18-00	19-00	20-10	21-30	22-30
31	493	411	358	318	289	19-30	21-00	22-40	0-10[a]	1-40[a]
33	502	419	367	328	298	19-50	21-20	23-00	0-20	1-30
35	507	423	370	332	301	19-40	21-20	23-00	0-30	2-00
37	504	421	368	329	298	20-00	21-50	23-40	1-20	2-50

[a]June 6, 1976

TABLE 4

COMPUTED AND OBSERVED TIMES[a]
FOR LEADING EDGE OF FLOOD WAVE

Location	Miles[b] downstream from dam	Observed Arrival Time (hours)	Computed arrival time n-values (hours) 0.03	0.04	0.05	0.06	0.07
At damsite	0.0	—	—	—	—	—	—
In Teton Canyon	3.0	1205	1206	1207	1208	1209	1210
At Teton	8.7	1230	1230	1230	1230	1240	1240
At Sugar City	12.9	1300	1340	1400	1420	1430	1440
At Rexburg	15.8	1340	1440	1500	1520	1530	1540
Henrys Fork near U.S.G.S. gaging station, Henrys Fork near Rexburg	21.1	1530	1540	1550	1650	1710	1740
Menan Bridge on the Snake River immediately upstream of the Union Pacific	27.6	1800	1730	1750	1830	1920	2030

[a]Times occurred on June 5, 1976.

[b]Distances based on the unsteady flow data model.

TABLE 5

COMPUTED AND OBSERVED PEAK DISCHARGES

Location	Miles[a] downstream from dam	Observed		Computed					
		Estimated time (hours)	Estimated discharge (cfs x 10^3)	Time (hours)	Discharge n-values (cfs x 10^3)				
					0.03	0.04	0.05	0.06	0.07
In Teton Canyon	3.0	1230-1330	2,300	1400-1410	1,850	1,820	1,785	1,730	1,700
At Teton	8.7	1300-1400	1,060	1420-1450	1,870	1,770	1,800	1,900	1,900

[a]Distances based on the unsteady flow data model.

TABLE 6

RESULTS OF UNSTEADY FLOW ANALYSIS
USING SIMULATED DISCHARGE HYDROGRAPH
FOR 40 PERCENT BREACH SIZE
(TRAPEZOIDAL SECTION)

Node No.	Maximum Elevation (feet above mean sea level)					Time of Maximum Elevation (hours - minutes)				
	n-values					n-values				
	0.03	0.04	0.05	0.06 [a]	0.07 [a]	0.03	0.04	0.05	0.06 [a]	0.07 [a]
1	5160.8	5174.8	5182.4	5193.8	5199.7	12-07	12-08	12-09	12-10	12-11
3	5132.8	5138.5	5142.5	5147.5	5155.7	12-10	12-11	12-12	12-13	12-14
5	5059.6	5068.2	5075.0	5081.1	5086.8	12-12	12-14	12-16	12-18	12-20
7	5013.1	5016.6	5019.8	5022.2	5023.2	12-26	12-30	12-40	12-40	12-40
9	4971.3	4973.5	4975.7	4976.6	4977.7	12-50	12-40	12-50	13-00	13-00
11	4951.3	4953.3	4954.4	4955.1	4956.1	12-50	13-00	13-10	13-20	13-20
13	4931.1	4932.0	4932.3	4933.4	4934.1	13-00	13-10	13-30	13-40	13-50
15	4910.3	4911.8	4912.3	4912.9	4913.3	13-10	13-30	13-50	14-00	14-20
17	4888.5	4889.5	4890.0	4890.5	4890.9	13-40	14-00	14-20	14-40	15-10
19	4866.3	4867.2	4867.9	4868.3	4868.6	14-10	14-40	15-10	15-40	16-10
21	4848.5	4849.3	4849.9	4850.4	4850.6	14-40	15-20	15-50	16-30	17-10
23	4838.5	4839.1	4839.5	4839.8	4840.0	15-10	16-00	16-40	17-30	18-10
25	4831.7	4832.1	4832.4	4832.7	4832.9	15-50	16-40	17-30	18-20	19-20
27	4824.3	4824.7	4825.0	4825.3	4825.5	17-10	18-20	19-30	20-40	22-00
29	4823.1	4823.4	4823.7	4823.9	4824.1	17-20	18-40	20-00	21-10	22-30
31	4819.1	4819.5	4819.8	4820.0	4820.1	17-50	19-10	20-40	22-10	23-30
33	4805.9	4806.3	4806.6	4806.8	4807.0	17-50	19-20	20-50	22-30	24-00
35	4791.5	4791.8	4792.0	4792.2	4792.3	18-00	19-40	21-20	22-50	0-20 [b]
37	4784.3	4784.6	4784.9	4785.1	4785.2	18-20	20-00	21-40	23-20	1-00

[a] Elevation table modified within the geometric model to accommodate the higher water surface elevations resulting from n values of 0.06 and 0.07.

[b] June 6, 1976

TABLE 6 (continued)

RESULTS OF UNSTEADY FLOW ANALYSIS
USING SIMULATED DISCHARGE HYDROGRAPH
FOR 40 PERCENT BREACH SIZE
(TRAPEZOIDAL SECTION)

Node No.	Maximum Discharge (cubic feet per second X 10^3)					Time of Maximum Discharge (hours - minutes)				
	n-values					n-values				
	0.03	0.04	0.05	0.06[a]	0.07[a]	0.03	0.04	0.05	0.06[a]	0.07[a]
1	3,353	3,353	3,353	3,353	3,353	12-01	12-01	12-01	12-01	12-01
3	5,225	4,697	4,191	3,864	3,802	12-10	12-11	12-12	12-05	12-05
5	4,311	4,498	4,457	4,447	4,369	12-12	12-13	12-15	12-16	12-17
7	2,712	2,575	2,396	2,412	2,322	12-25	12-30	12-40	12-40	12-40
9	2,491	2,606	2,482	2,144	2,208	12-50	12-40	12-50	13-00	13-00
11	2,693	2,629	2,600	2,543	2,395	12-50	13-00	13-00	13-10	13-20
13	2,961	2,743	2,321	2,032	1,881	13-00	13-10	13-20	13-30	13-50
15	3,107	2,722	2,215	2,135	1,879	13-10	13-30	13-40	14-00	14-10
17	2,466	2,287	2,035	1,824	1,659	13-40	14-00	14-20	14-40	15-00
19	1,932	1,659	1,472	1,308	1,158	14-10	14-30	15-00	15-30	16-00
21	1,508	1,271	1,071	951	840	14-30	15-10	15-40	16-20	16-50
23	1,128	902	782	680	599	15-00	15-40	16-30	17-10	17-50
25	765	637	547	480	429	15-40	16-30	17-20	18-10	18-50
27	731	599	506	438	386	15-50	16-50	17-50	18-50	19-40
29	551	445	375	325	286	16-20	17-30	18-30	19-30	20-30
31	500	399	332	285	251	17-50	19-20	20-40	22-10	22-10
33	515	416	350	303	267	17-40	19-10	20-50	22-10	23-40
35	521	419	352	305	269	18-00	19-40	21-10	22-40	0-10[b]
37	517	416	349	302	266	19-20	20-00	21-40	23-20	1-00

[a]Elevation table modified within the geometric model to accommodate the higher water surface elevations resulting from n values of 0.06 and 0.07.

[b]June 6, 1976.

location of the odd numbered computation points and conveyance limits are shown (a discussion of the conveyance limits is contained in the users manual for the GEDA program). (It is apparent from Plate 10 that the majority of high water mark observations are along the edges of the flooded area.) Maximum water surface elevations are plotted in Plates 11, 12 and 13.

The observed high water marks (taken from Plate 10) were plotted in Plates 11, 12 and 13 and designated as left or right bank (looking downstream). The ground profile shown reflects the minimum elevation in the various cross sections used in the geometric model. Horizontal distances are measured along the most probable path of concentrated flow and not along any particular tributary as shown in Plate 10. The spacing and location of the odd numbered nodes are also included in the profile plots. Maximum water surface elevations computed in the simulation of observed data were plotted for the odd numbered nodes shown. Water surface profiles were then drawn for each n value used in the analysis.

If a number of cross sections are drawn on Plate 10 normal to estimated flow lines, particularly in the area of Rexburg where floodwaters tended to spread laterally, a significant variation in high water mark elevations between the left and right banks of a given cross section is apparent. In some instances, the difference is as much as 30 feet. This situation is also apparent in Plates 11, 12 and 13. In general, where floodwaters were relatively confined between the left and right banks, elevations of high water marks on opposite sides are essentially the same.

A comparison of the observed and computed maximum water surface elevations (Plates 11, 12 and 13) would seem to indicate the following:

(1) Floodwaters were probably concentrated in the center of the flooded area between the U.S.G.S. gaging station on the Teton River and the downstream limits of Sugar City (see Plate 10).

(2) Floodwaters were probably concentrated in the vicinity of Rexburg.

It is difficult to analyze the accuracy of the computed results based on observed high water marks. Any detailed analysis would definitely require high water marks within the limits of flooding. If such could be obtained a greater effort could be made in stipulating conveyance limits and in the actual calibration of an unsteady flow model.

Tables 1 and 4 compare the estimated (based on field observations) and computed arrival times of the leading edge of the flood wave, whereas Tables 2 and 5 compare estimated (based on field observations) and computed maximum discharges at particular locations within the study area. Plate 14 gives an indication of the time required for passage of the flood wave (based on n=0.04).

In the unsteady flow model, determination of the arrival time of the leading edge of the flood wave depends on a noticeable difference in the computed water surface elevation occurring at a given node. Since minor fluctuations of the water surface were present in the base flow and since the printout interval was 10 minutes after 12:30 p.m., arrival times were estimated (probably ± 30 minutes).

Computed peak discharges (Table 5) differ significantly from those estimated from observed data (Table 2). It is reasonable to assume though that the discharges of Table 2 are only rough approximations.

In the development of the unsteady flow data model, there was no effort made to locate computation points at those locations specified in Tables 1 and 2. (Usually, computation points are located such that results are printed at desired locations.)

5. STEADY FLOW MODEL

The information originally coded in the HEC-2 format and utilized in development of the channel geometric model, was used to determine the storage-outflow relationships for various reaches downstream of the dam. Multiple profiles were run using HEC-2 and the volumes in a given reach, corresponding to a specified discharge, computed. (It should be noted that an n-value of 0.04 was used in the multiple profile computations.)

The discharge hydrograph (see Plate 6) based on observed data, was routed downstream with the storage-outflow relationships previously determined. Channel routing was accomplished with HEC-1[1] using modified Puls. The peak discharges computed for each reach were subsequently input into the HEC-2 data deck.

Before running, the HEC-2 deck was modified to reflect the conveyance limits adopted in the unsteady flow analysis (see Plate 10). Encroachment limits were set with the X3 card as close as possible to the conveyance limits previously designated (this was necessary since GR stations did not always correspond to the conveyance limits specified in the geometric data model). The resulting water surface profile is shown in Plates 15, 16 and 17 (superimposed for comparison).

The difference in the computed water surface profiles between the two methods (the steady flow and the unsteady flow analysis) is due, in part, to the difference in the computed discharges. Discharges computed using modified Puls were lower in the upstream channel reaches and higher in the lower reaches. This is attributed to the significant effect of the inertia component (in the unsteady model) immediately downstream of the dam and in the way storage is treated in the two methods.

---

[1] HEC-1 Flood Hydrograph Package, Generalized Computer Program (723-010), Hydrologic Engineering Center, U.S. Army Corps of Engineers, January 1973.

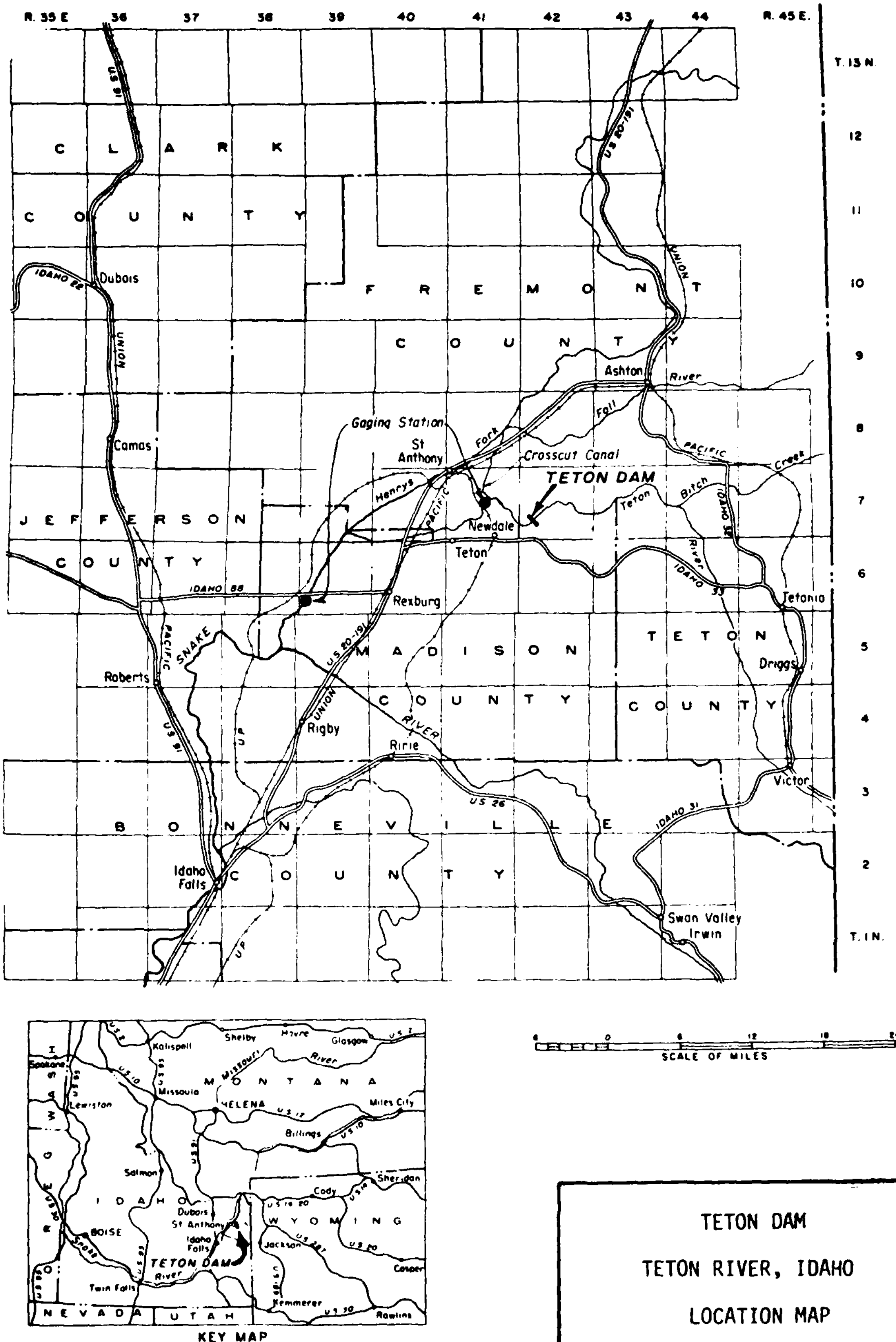

TETON DAM

TETON RIVER, IDAHO

LOCATION MAP

PLATE 1

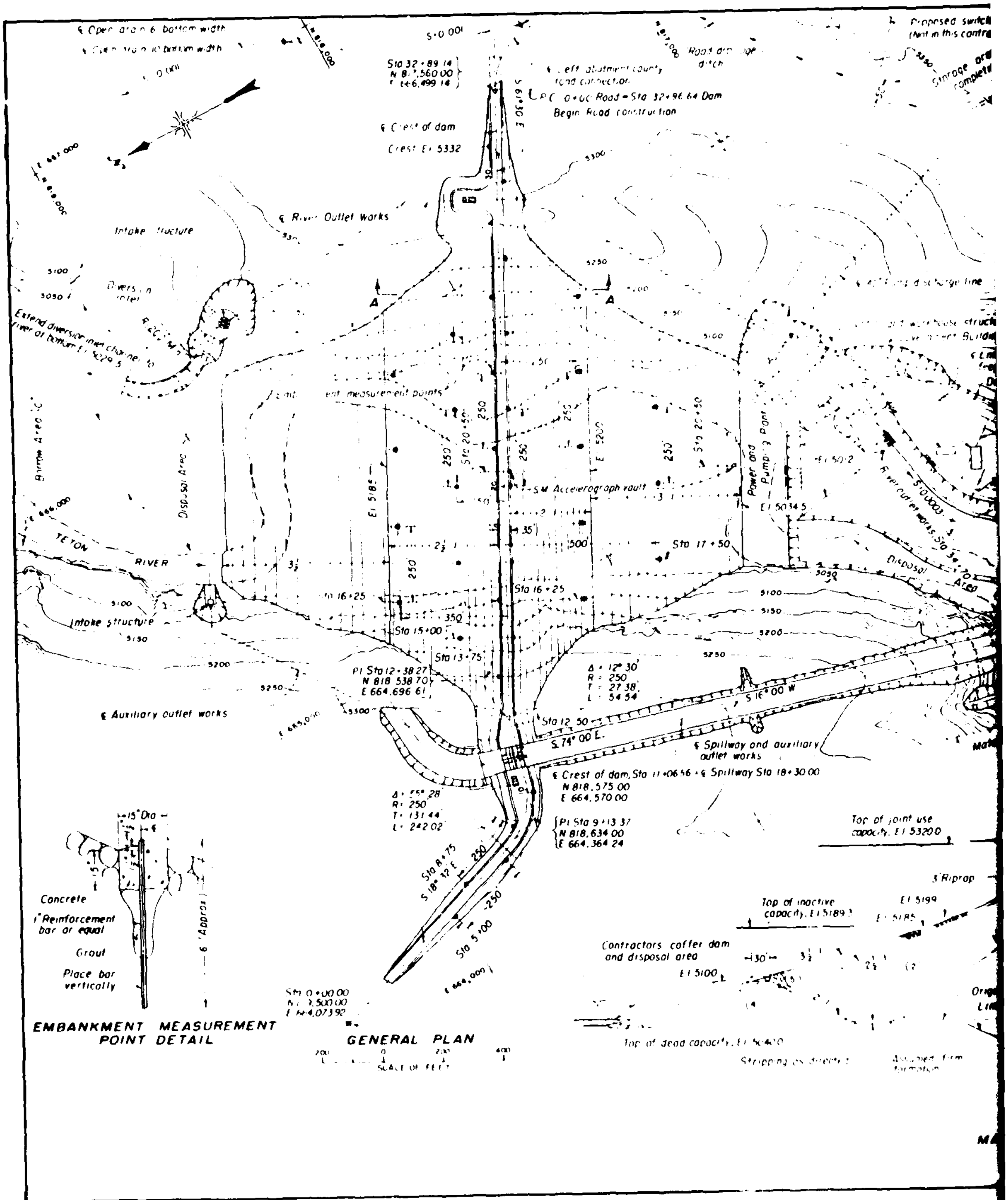

EMBANKMENT MEASUREMENT POINT DETAIL

GENERAL PLAN

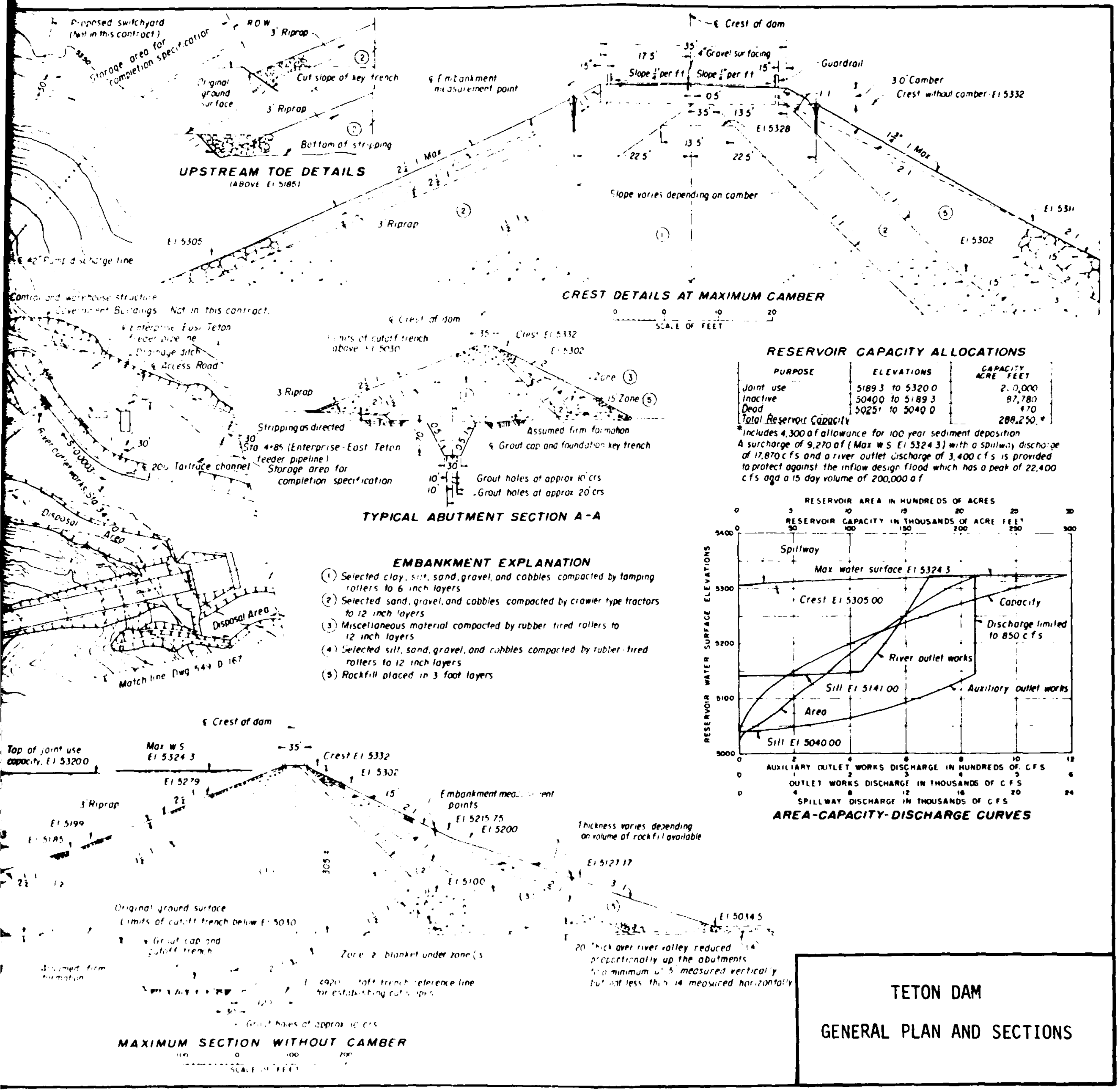

RESERVOIR CAPACITY ALLOCATIONS

PURPOSE	ELEVATIONS	CAPACITY ACRE FEET
Joint use	5189.3 to 5320.0	200,000
Inactive	5040.0 to 5189.3	87,780
Dead	5025± to 5040.0	470
Total Reservoir Capacity		288,250*

*Includes 4,300 a.f. allowance for 100 year sediment deposition.
A surcharge of 9,270 a.f. (Max W.S. El 5324.3) with a spillway discharge of 17,870 c.f.s. and a river outlet discharge of 3,400 c.f.s. is provided to protect against the inflow design flood which has a peak of 22,400 c.f.s. and a 15 day volume of 200,000 a.f.

EMBANKMENT EXPLANATION

(1) Selected clay, silt, sand, gravel, and cobbles compacted by tamping rollers to 6 inch layers
(2) Selected sand, gravel, and cobbles compacted by crawler type tractors to 12 inch layers
(3) Miscellaneous material compacted by rubber tired rollers to 12 inch layers
(4) Selected silt, sand, gravel, and cobbles compacted by rubber tired rollers to 12 inch layers
(5) Rockfill placed in 3 foot layers

TETON DAM

GENERAL PLAN AND SECTIONS

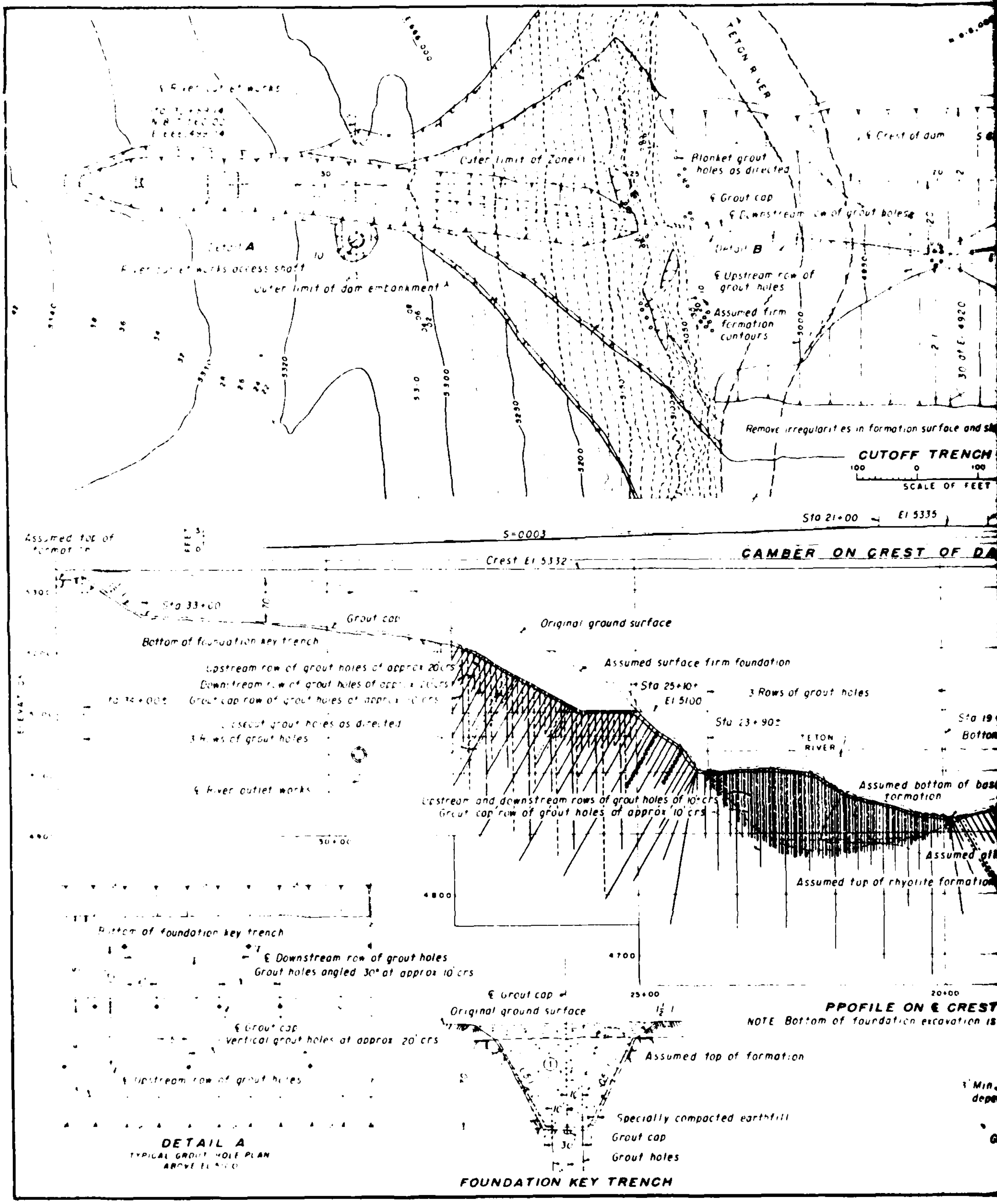

TETON RIVER
℄ Crest of dam
Outer limit of Zone 1
Blanket grout holes as directed
℄ Grout cap
Detail A
Detail B
River outlet works access shaft
Outer limit of dam embankment
℄ Upstream row of grout holes
Assumed firm formation contours
CUTOFF TRENCH
SCALE OF FEET
Sta 21+00
El 5335
S=0.003
Crest El 5332
Sta 33+00
Grout cap
Original ground surface
Bottom of foundation key trench
Assumed surface firm foundation
Upstream row of grout holes of approx 20' crs
Sta 25+10±
El 5100
3 Rows of grout holes
Sta 23+90±
TETON RIVER
℄ River outlet works
Upstream and downstream rows of grout holes of 10' crs
Grout cap row of grout holes of approx 10' crs
Assumed top of rhyolite formation
4800
4700
25+00
20+00
Bottom of foundation key trench
℄ Downstream row of grout holes
Grout holes angled 30° at approx 10' crs
℄ Grout cap
Vertical grout holes at approx 20' crs
℄ Upstream row of grout holes
DETAIL A
℄ Grout cap
Original ground surface
Assumed top of formation
Specially compacted earthfill
Grout cap
Grout holes
FOUNDATION KEY TRENCH

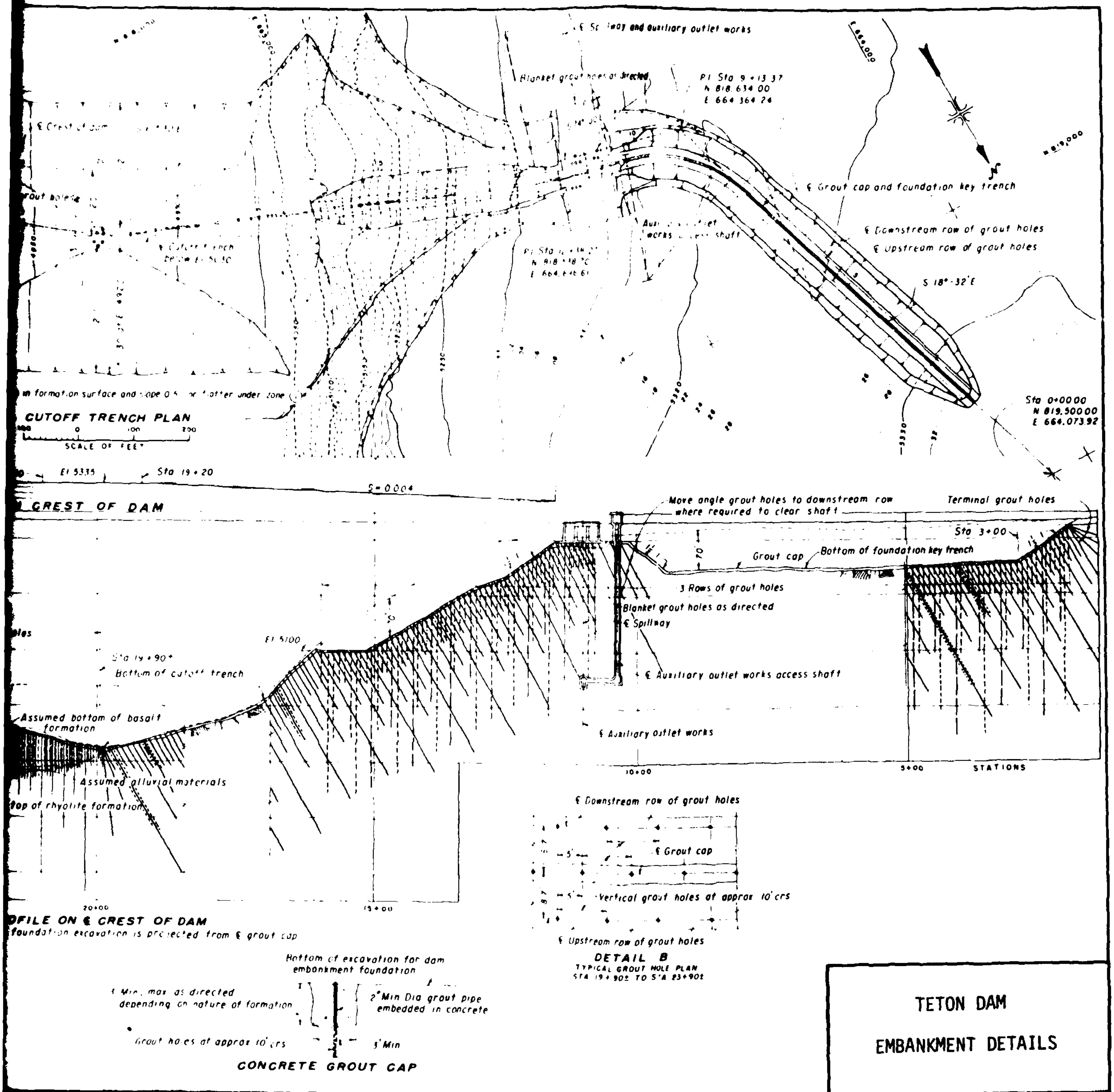

TETON DAM

EMBANKMENT DETAILS

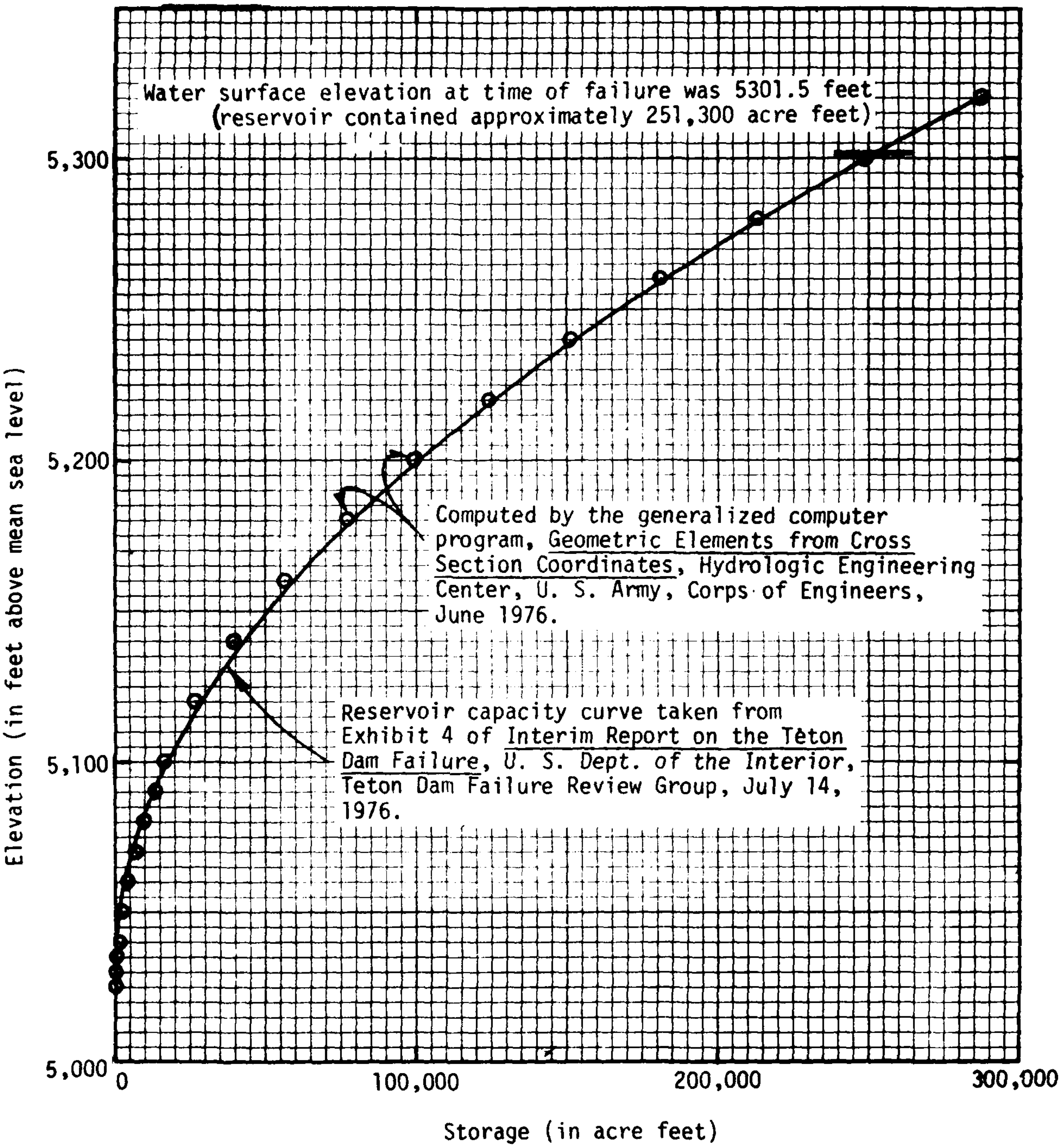

TETON DAM

RESERVOIR CAPACITY

Storage versus Elevation

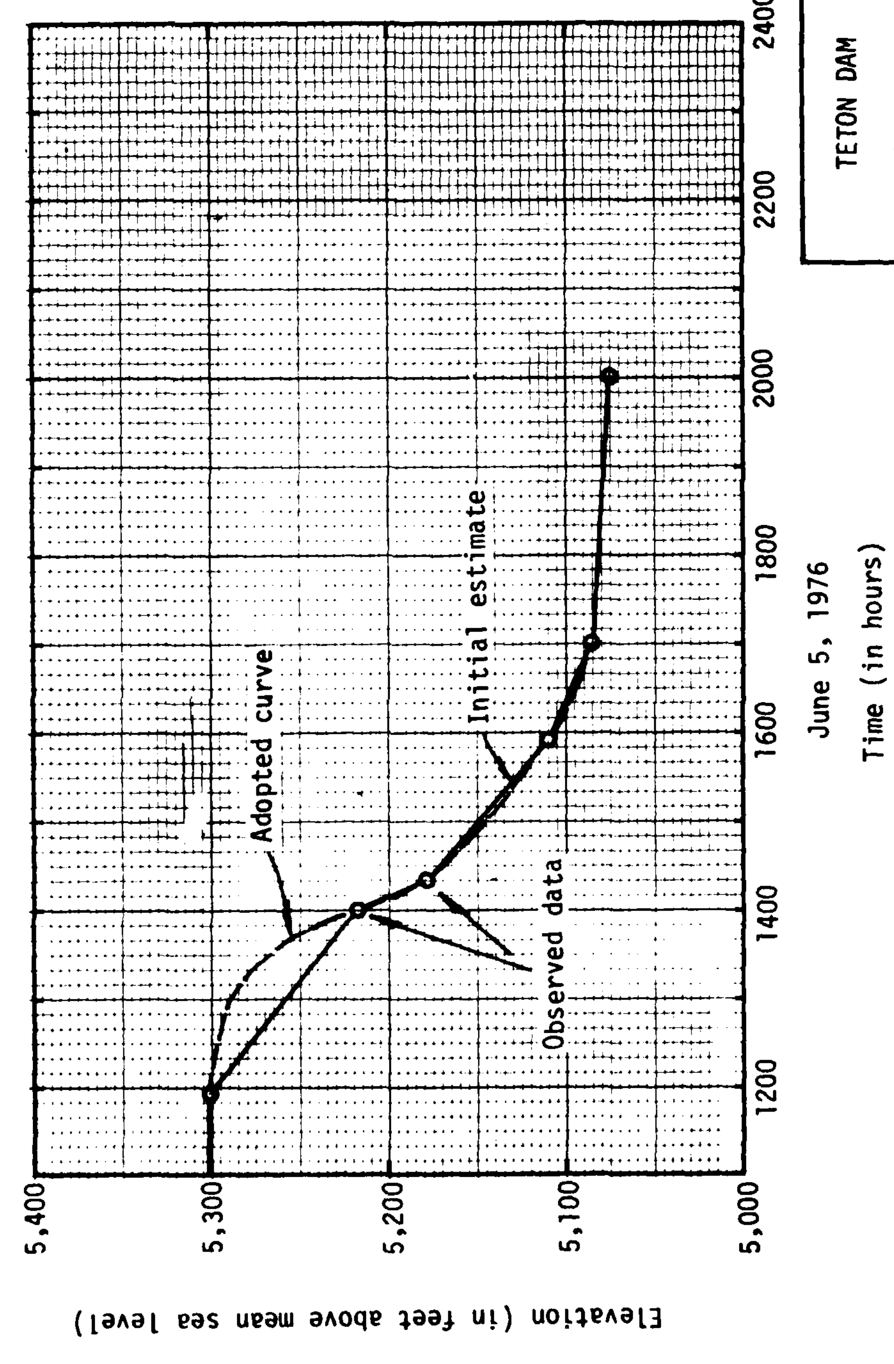

TETON DAM
ELEVATION HYDROGRAPH
FOR RESERVOIR

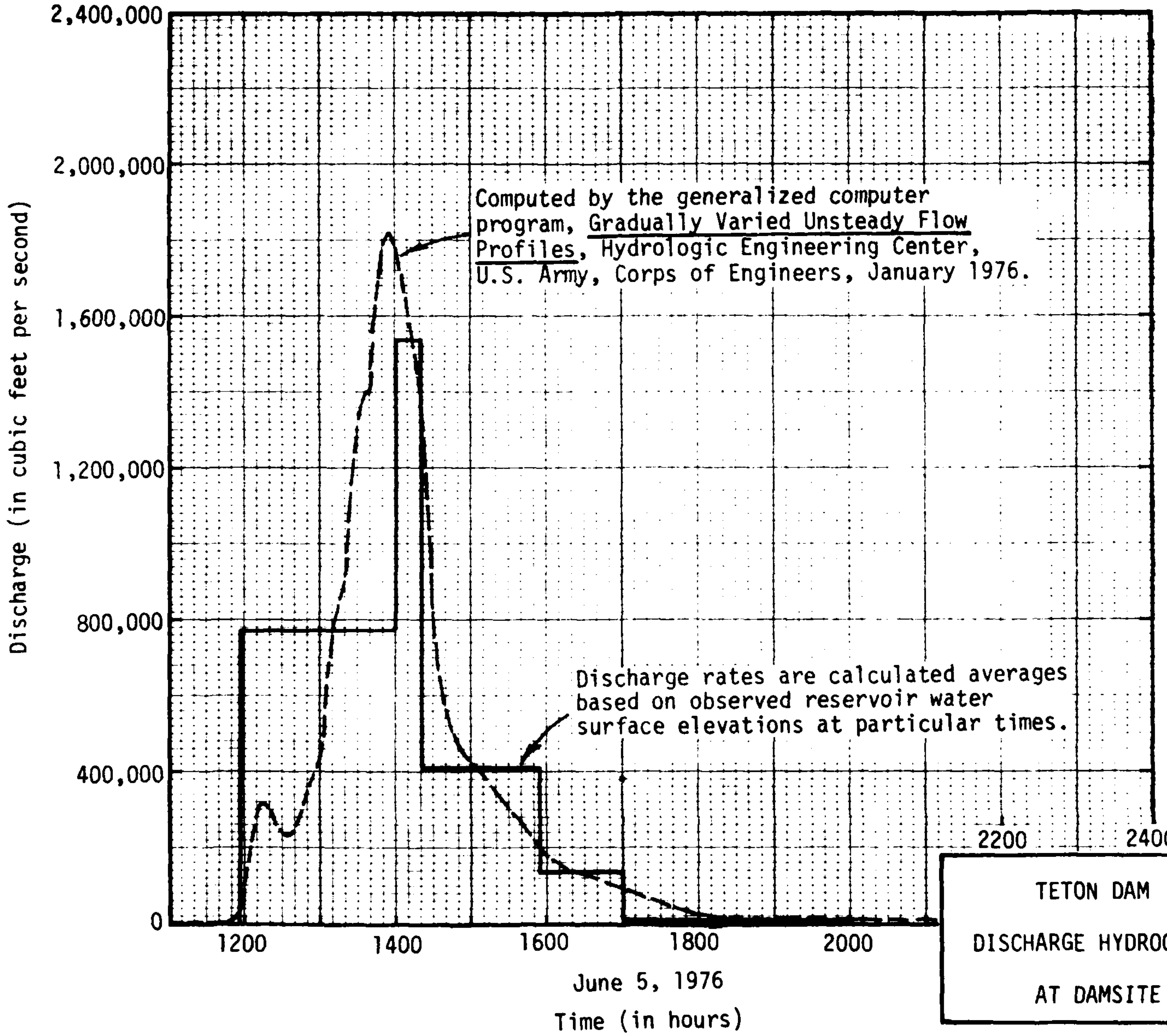

TETON DAM

DISCHARGE HYDROGRAPH

AT DAMSITE

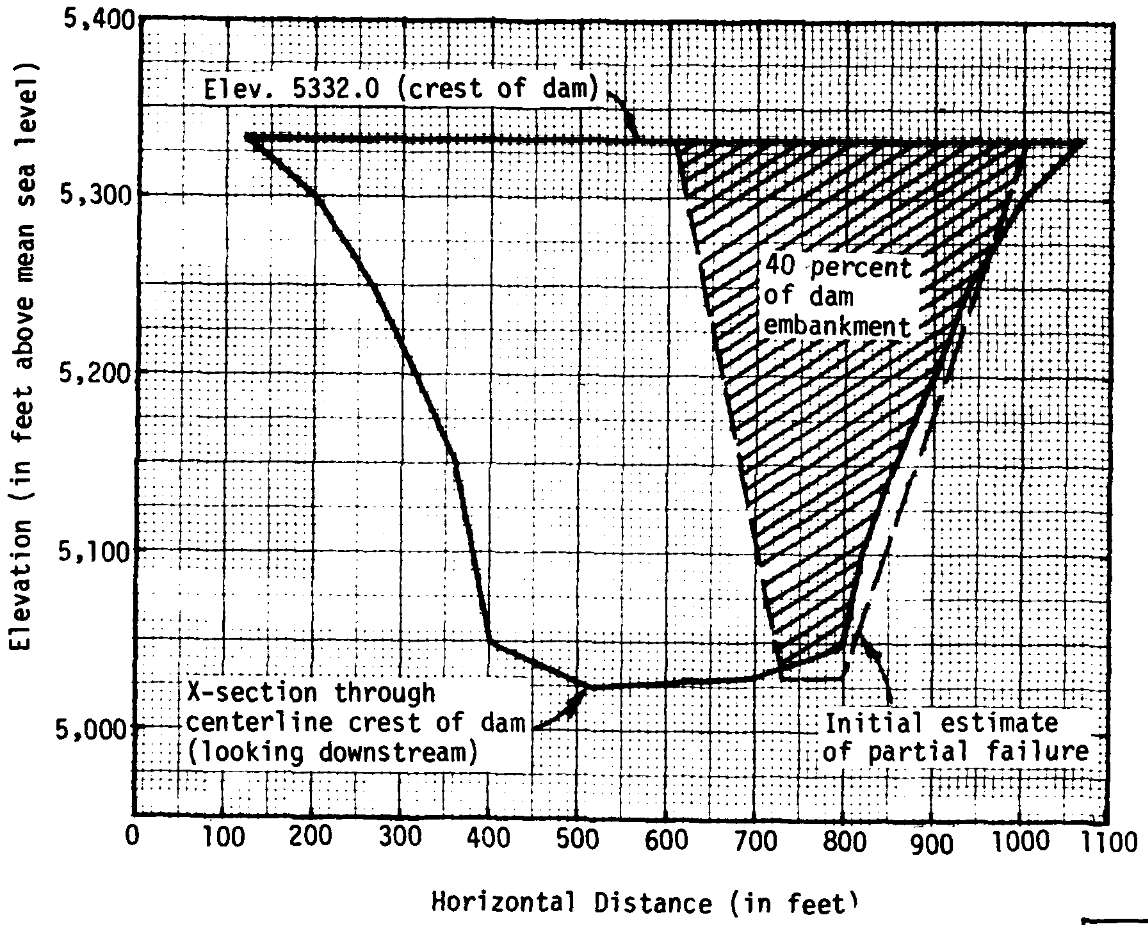

TETON DAM

INITIAL ESTIMATE OF
PARTIAL FAILURE

TRAPEZOIDAL SECTION

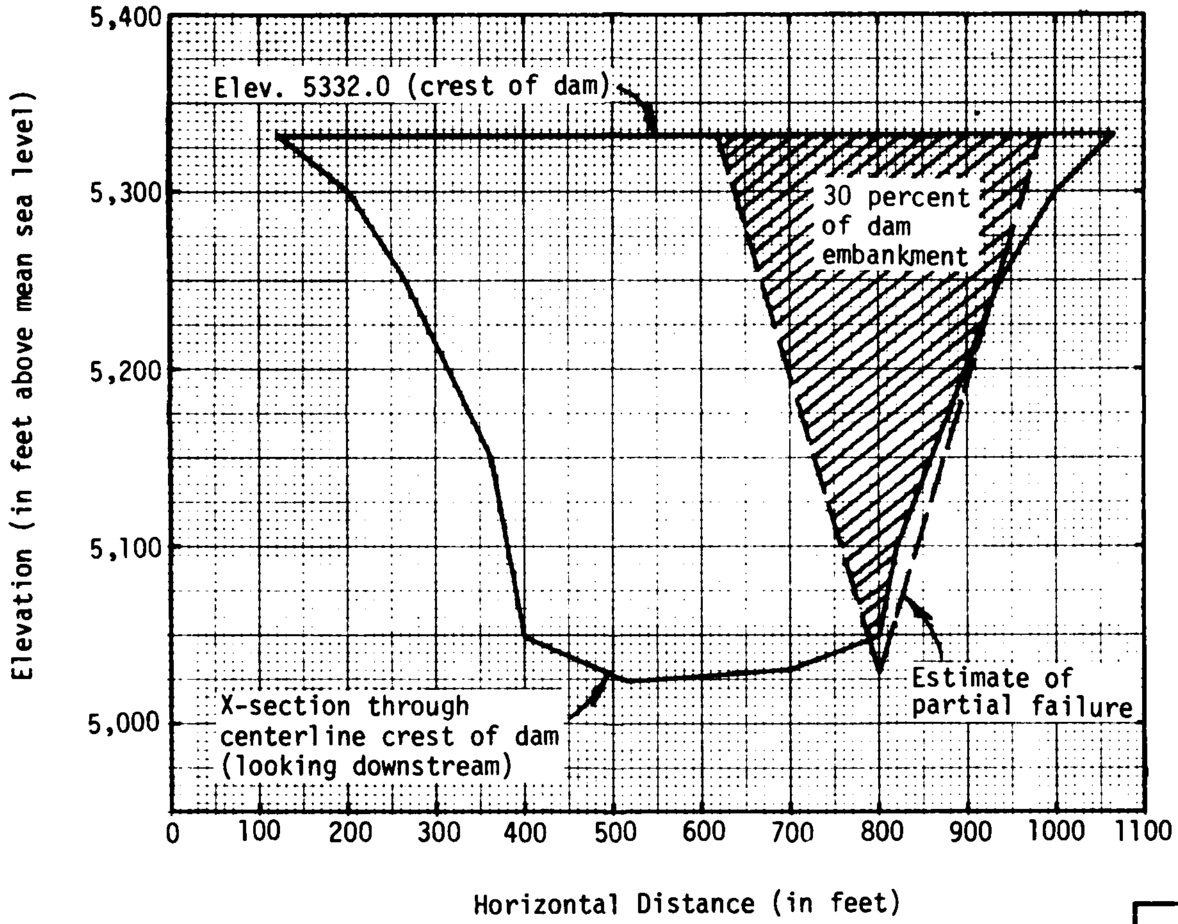

TETON DAM

ESTIMATE
OF PARTIAL FAILURE

TRIANGULAR SECTION

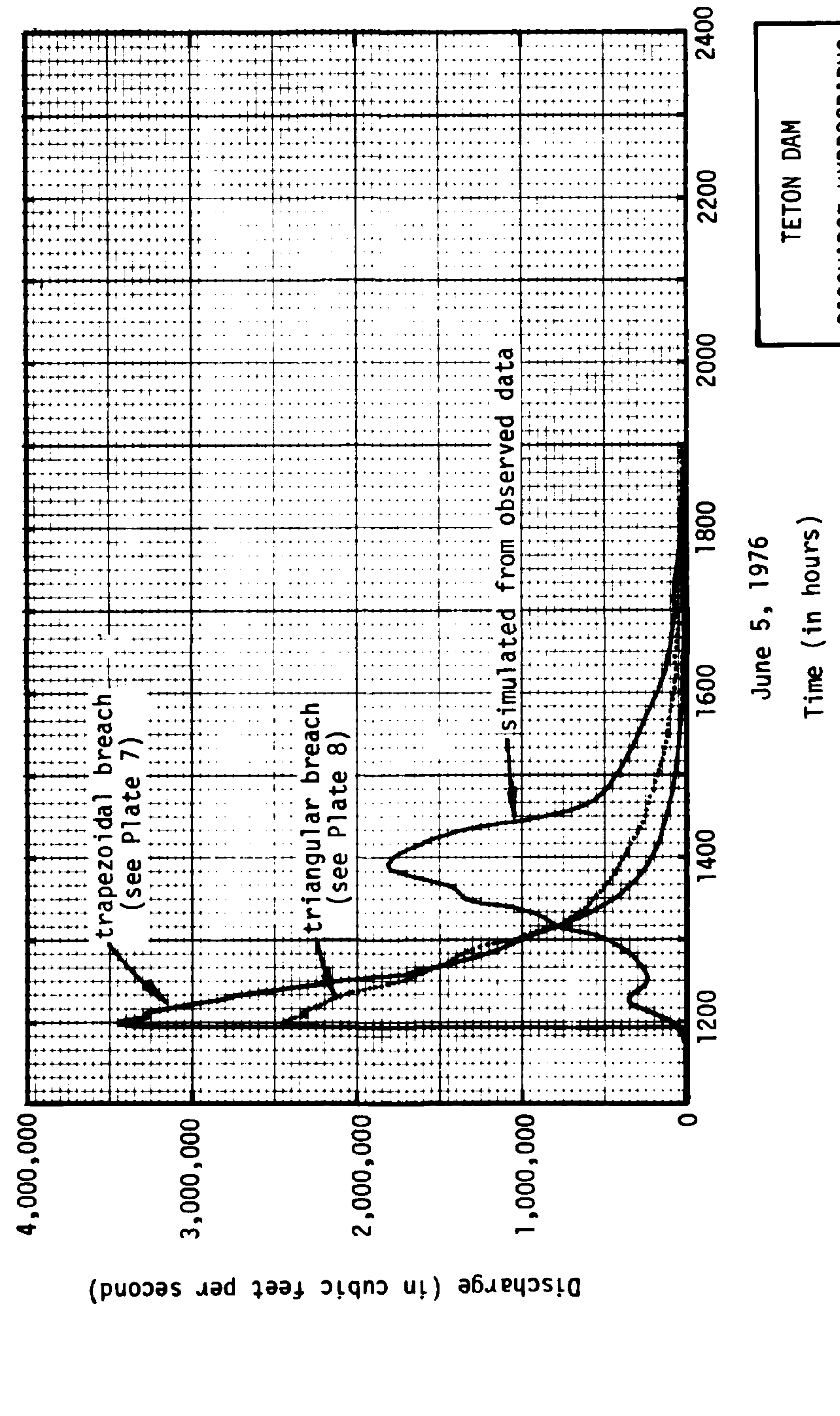

TETON DAM
DISCHARGE HYDROGRAPHS
AT DAMSITE

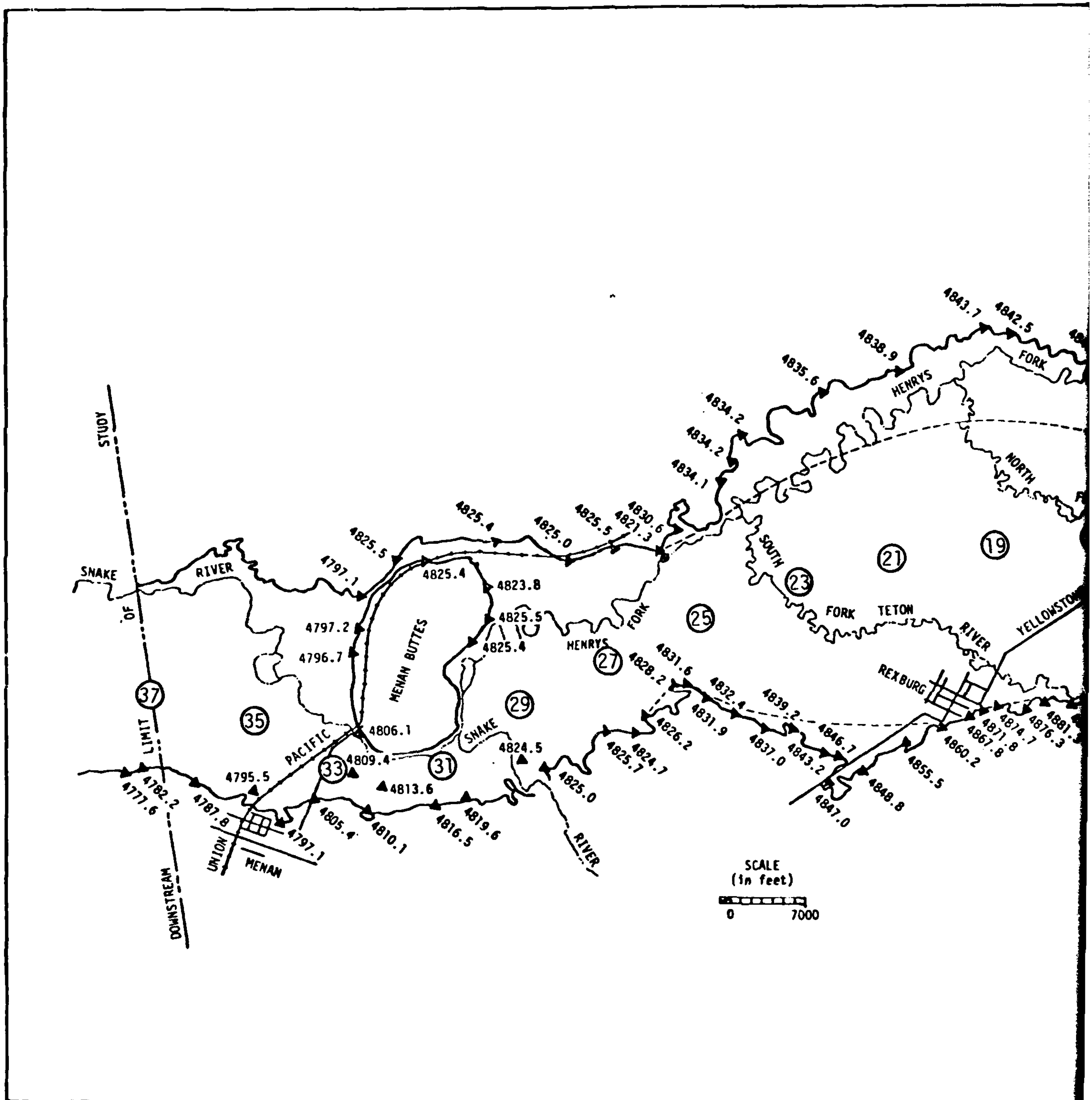
STUDY
LIMIT
OF
DOWNSTREAM
SNAKE
RIVER
MENAN BUTTES
PACIFIC
UNION
MENAN
SNAKE
RIVER
HENRYS
FORK
SOUTH
FORK
TETON
RIVER
NORTH
HENRYS
FORK
REXBURG
YELLOWSTONE
SCALE
(in feet)
0
7000
37
35
33
31
29
27
25
23
21
19
4777.6
4782.2
4787.8
4795.5
4797.1
4805.4
4810.1
4816.5
4819.6
4813.6
4809.4
4806.1
4796.7
4797.2
4797.1
4825.5
4825.4
4823.8
4825.5
4825.4
4825.4
4825.0
4825.5
4821.3
4830.6
4824.5
4825.0
4825.7
4824.7
4826.2
4828.2
4831.6
4831.9
4832.4
4837.0
4839.2
4843.2
4846.7
4847.0
4848.8
4855.5
4860.2
4867.8
4871.8
4874.7
4876.3
4834.1
4834.2
4834.2
4835.6
4838.9
4843.7
4842.5

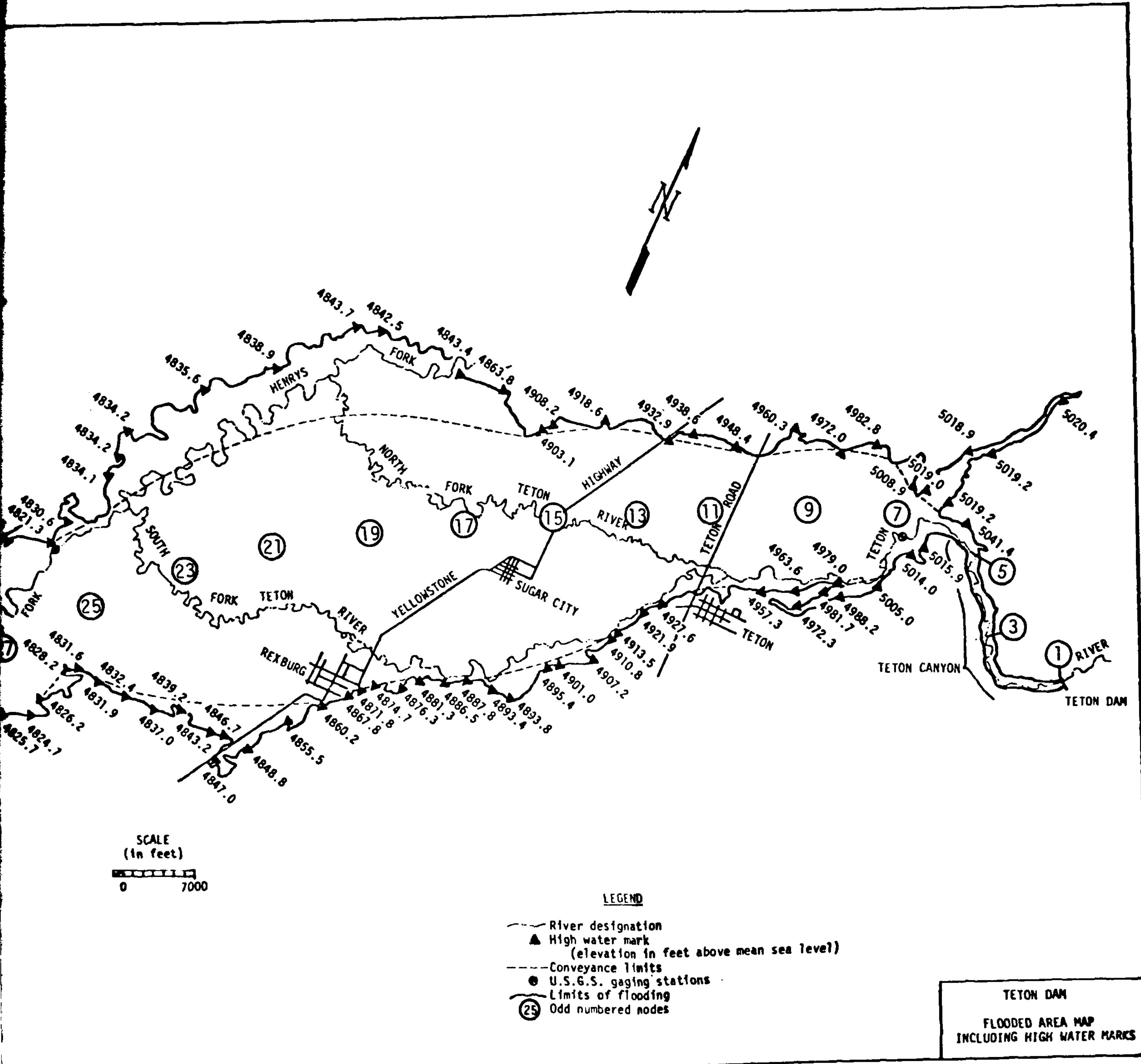
HENRYS
FORK
NORTH
FORK
TETON
RIVER
SOUTH
FORK
TETON
RIVER
HIGHWAY
YELLOWSTONE
SUGAR CITY
REXBURG
TETON ROAD
TETON
TETON CANYON
TETON DAM
RIVER
SCALE
(in feet)
0
7000
LEGEND
River designation
High water mark
(elevation in feet above mean sea level)
Conveyance limits
U.S.G.S. gaging stations
Limits of flooding
Odd numbered nodes
TETON DAM
FLOODED AREA MAP
INCLUDING HIGH WATER MARKS

PLATE 10

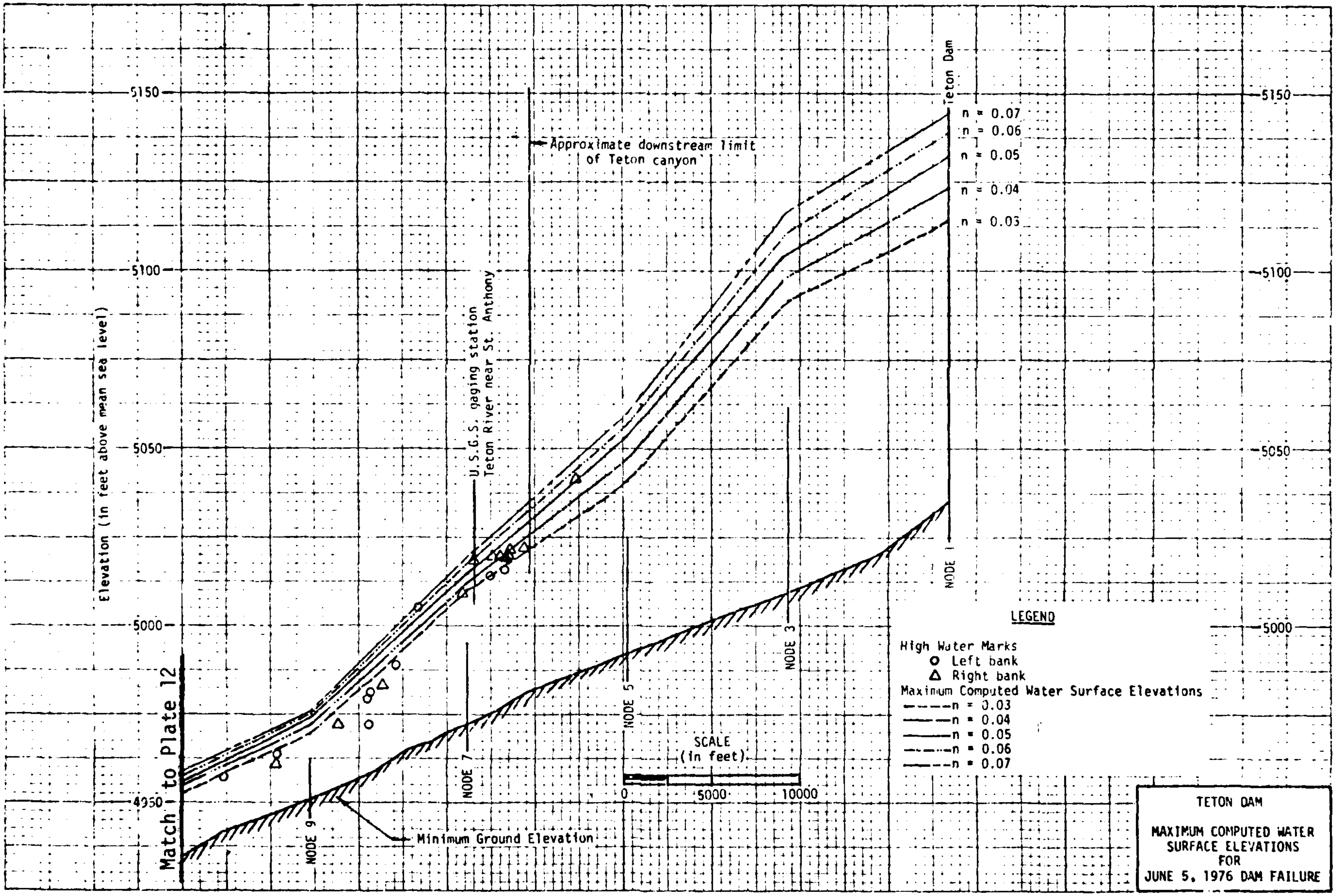
Elevation (in feet above mean sea level)
5150
5100
5050
5000
4950
Teton Dam
n = 0.07
n = 0.06
n = 0.05
n = 0.04
n = 0.03
Approximate downstream limit of Teton canyon
U.S.G.S. gaging station Teton River near St. Anthony
NODE 1
NODE 3
NODE 5
NODE 7
NODE 9
Minimum Ground Elevation
Match to Plate 12
SCALE (in feet)
0
5000
10000
LEGEND
High Water Marks
O Left bank
Δ Right bank
Maximum Computed Water Surface Elevations
n = 0.03
n = 0.04
n = 0.05
n = 0.06
n = 0.07
TETON DAM
MAXIMUM COMPUTED WATER SURFACE ELEVATIONS FOR JUNE 5, 1976 DAM FAILURE

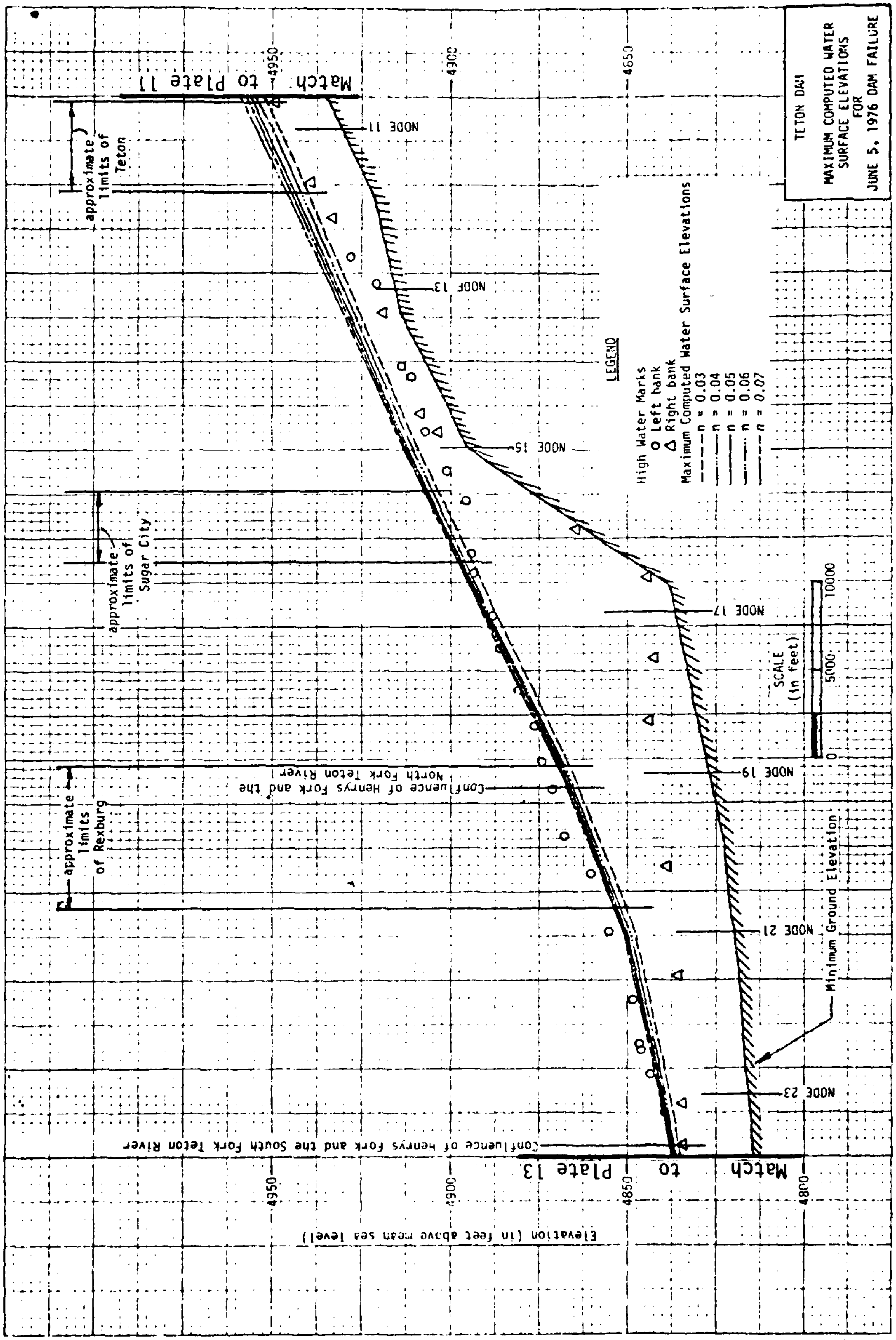
TETON DAM
MAXIMUM COMPUTED WATER SURFACE ELEVATIONS FOR JUNE 5, 1976 DAM FAILURE
LEGEND
High Water Marks
o Left bank
Δ Right bank
Maximum Computed Water Surface Elevations
n = 0.03
n = 0.04
n = 0.05
n = 0.06
n = 0.07
SCALE (in feet)
0
5000
10000
Match to Plate 11
Match to Plate 13
approximate limits of Teton
approximate limits of Sugar City
approximate limits of Rexburg
Confluence of Henrys Fork and the North Fork Teton River
Confluence of Henrys Fork and the South Fork Teton River
NODE 11
NODE 13
NODE 15
NODE 17
NODE 19
NODE 21
NODE 23
Minimum Ground Elevation
Elevation (in feet above mean sea level)
4950
4900
4850
4800

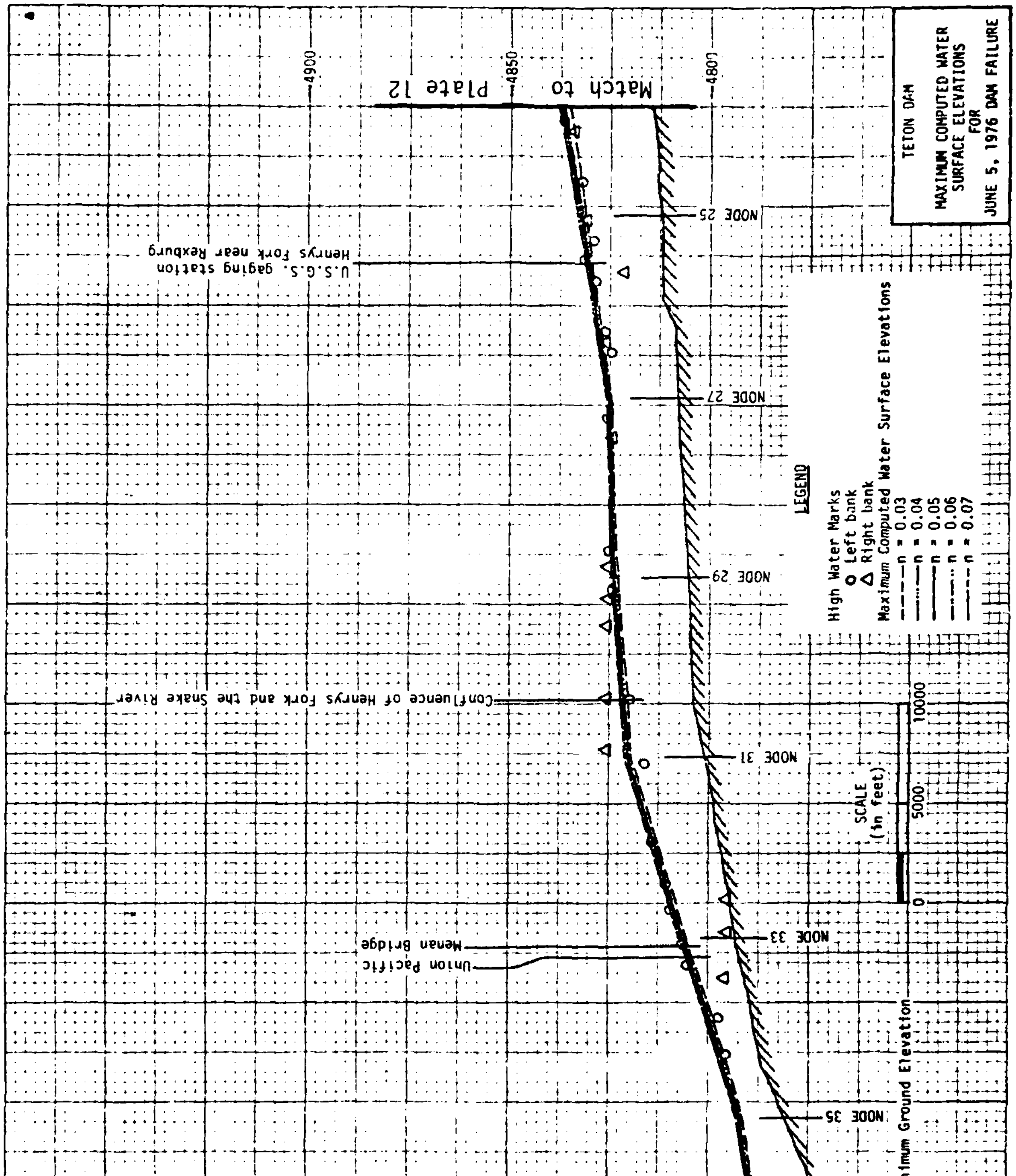
TETON DAM
MAXIMUM COMPUTED WATER
SURFACE ELEVATIONS
FOR
JUNE 5, 1976 DAM FAILURE
LEGEND
High Water Marks
O Left bank
Δ Right bank
Maximum Computed Water Surface Elevations
n = 0.03
n = 0.04
n = 0.05
n = 0.06
n = 0.07
SCALE
(in feet)
0
5000
10000
Match to Plate 12
NODE 25
U.S.G.S. gaging station
Henrys Fork near Rexburg
NODE 27
NODE 29
Confluence of Henrys Fork and the Snake River
NODE 31
NODE 33
Menan Bridge
Union Pacific
NODE 35
Minimum Ground Elevation
NODE 37
Downstream limit of study
Elevation (in feet above mean sea level)
4900
4850
4800
4750

PLATE 13

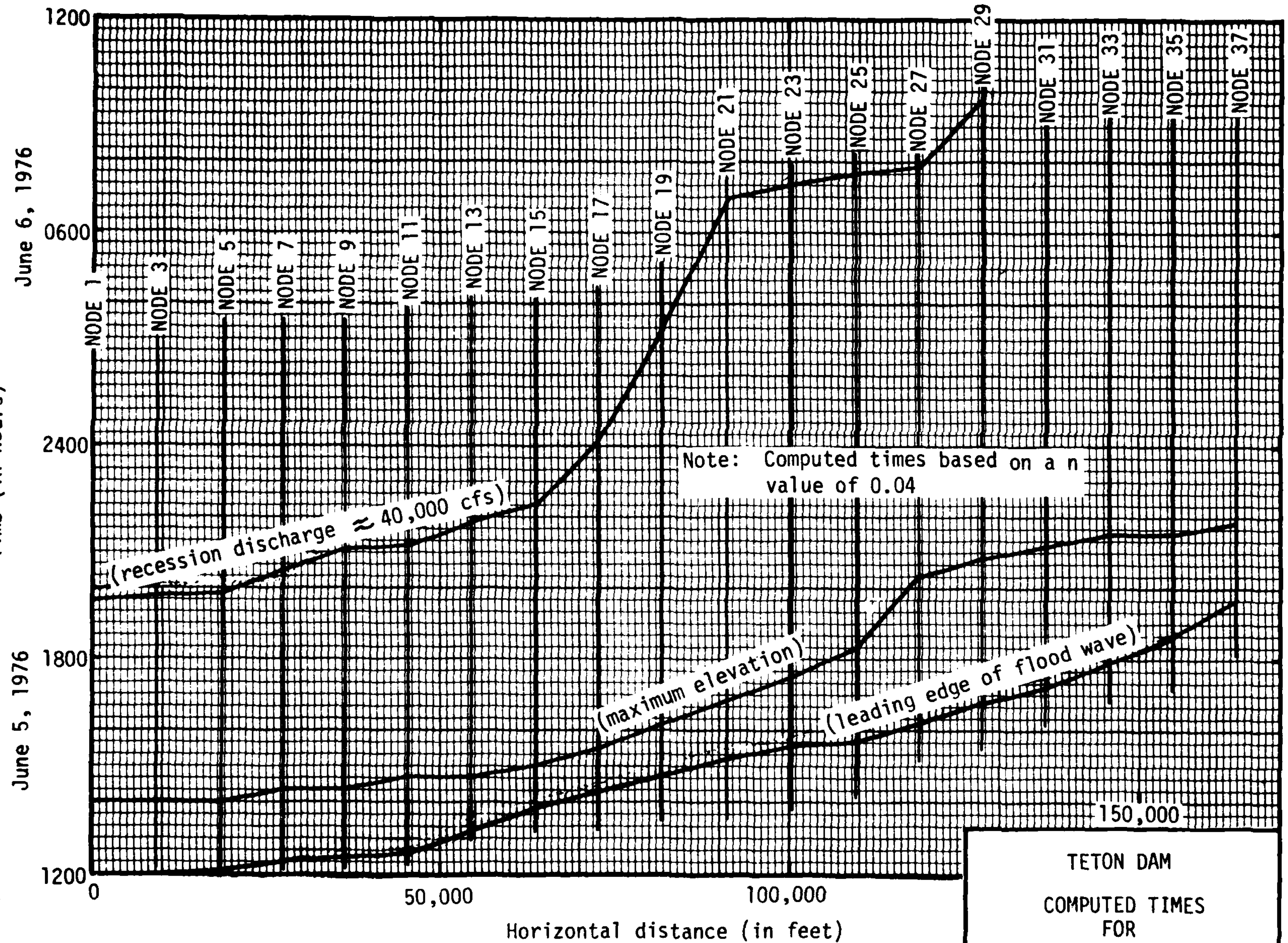

TETON DAM

COMPUTED TIMES
FOR
JUNE 5, 1976 DAM FAILURE

PLATE 14

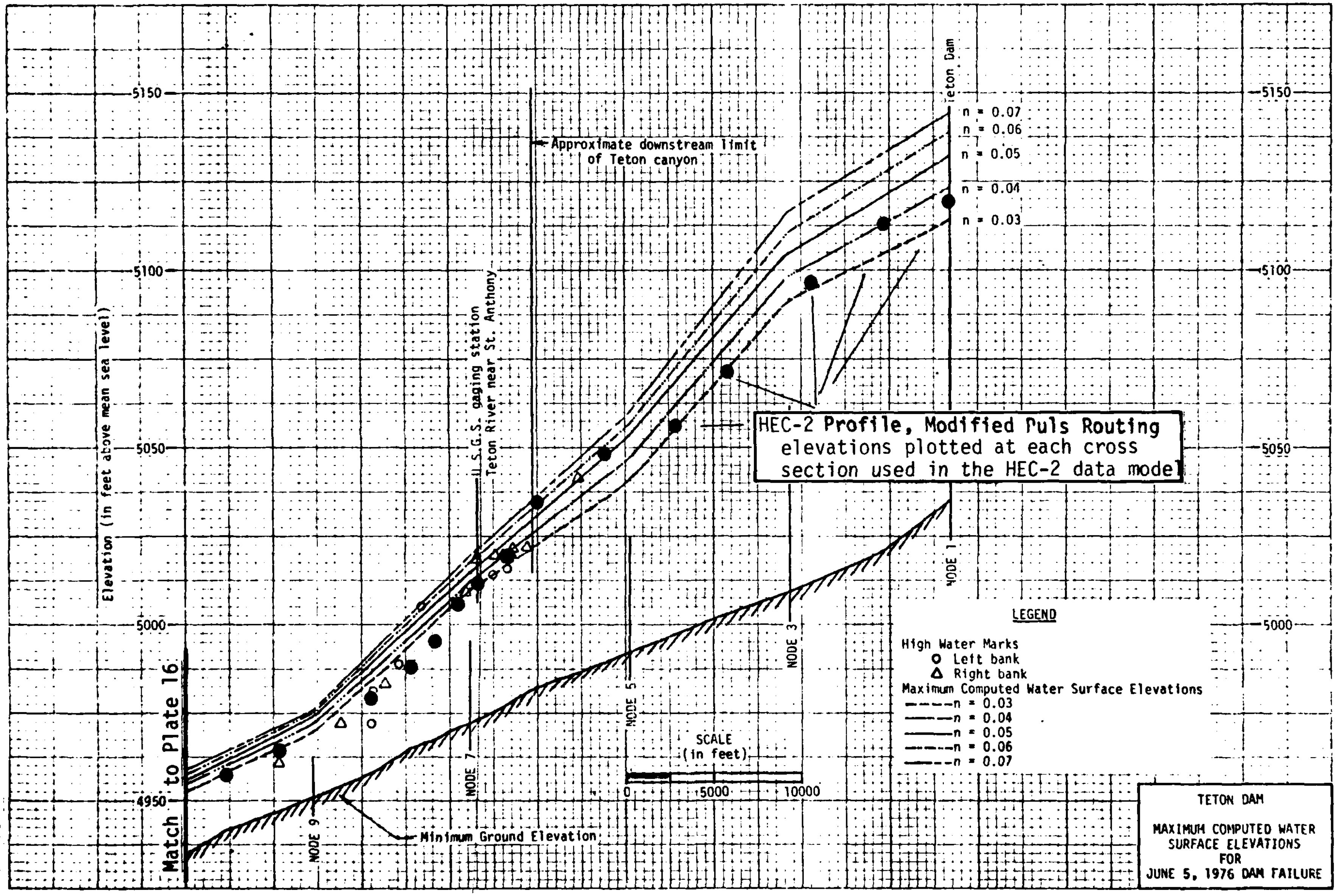

Teton Dam
n = 0.07
n = 0.06
n = 0.05
n = 0.04
n = 0.03
Approximate downstream limit of Teton canyon
U.S.G.S. gaging station Teton River near St. Anthony
HEC-2 Profile, Modified Puls Routing elevations plotted at each cross section used in the HEC-2 data model
Elevation (in feet above mean sea level)
5150
5100
5050
5000
4950
NODE 1
NODE 3
NODE 5
NODE 7
NODE 9
Minimum Ground Elevation
Match to Plate 16
SCALE (in feet)
0
5000
10000
LEGEND
High Water Marks
Left bank
Right bank
Maximum Computed Water Surface Elevations
n = 0.03
n = 0.04
n = 0.05
n = 0.06
n = 0.07
TETON DAM
MAXIMUM COMPUTED WATER SURFACE ELEVATIONS FOR JUNE 5, 1976 DAM FAILURE

PLATE 15

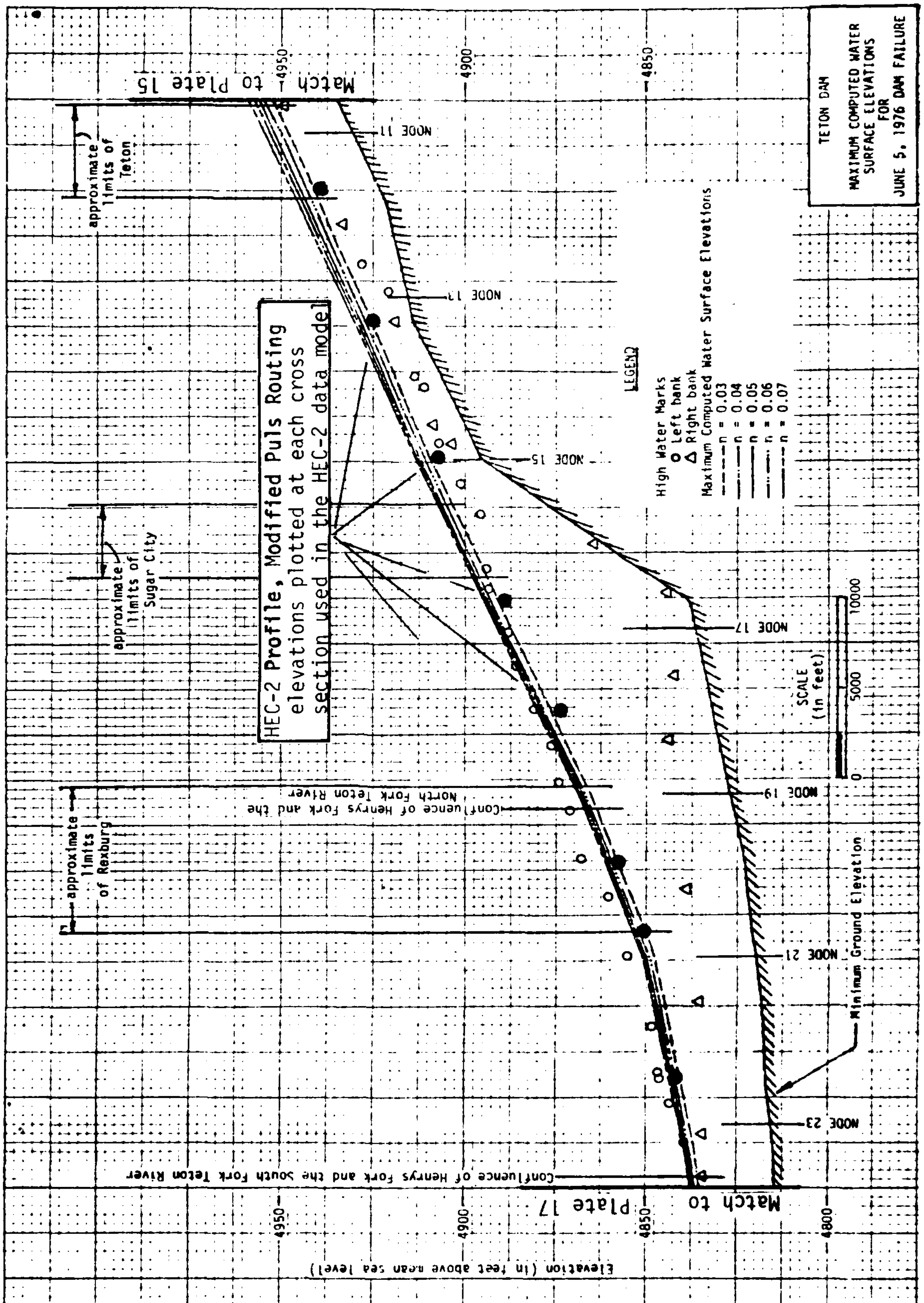
TETON DAM
MAXIMUM COMPUTED WATER SURFACE ELEVATIONS FOR JUNE 5, 1976 DAM FAILURE
Match to Plate 15
Match to Plate 17
4950
4900
4850
4800
Elevation (in feet above mean sea level)
NODE 11
NODE 13
NODE 15
NODE 17
NODE 19
NODE 21
NODE 23
approximate limits of Teton
approximate limits of Sugar City
approximate limits of Rexburg
HEC-2 Profile, Modified Puls Routing elevations plotted at each cross section used in the HEC-2 data model
Confluence of Henrys Fork and the North Fork Teton River
Confluence of Henrys Fork and the South Fork Teton River
Minimum Ground Elevation
LEGEND
High Water Marks
o Left bank
Δ Right bank
Maximum Computed Water Surface Elevations
n = 0.03
n = 0.04
n = 0.05
n = 0.06
n = 0.07
SCALE (in feet)
0
5000
10000

PLATE 16

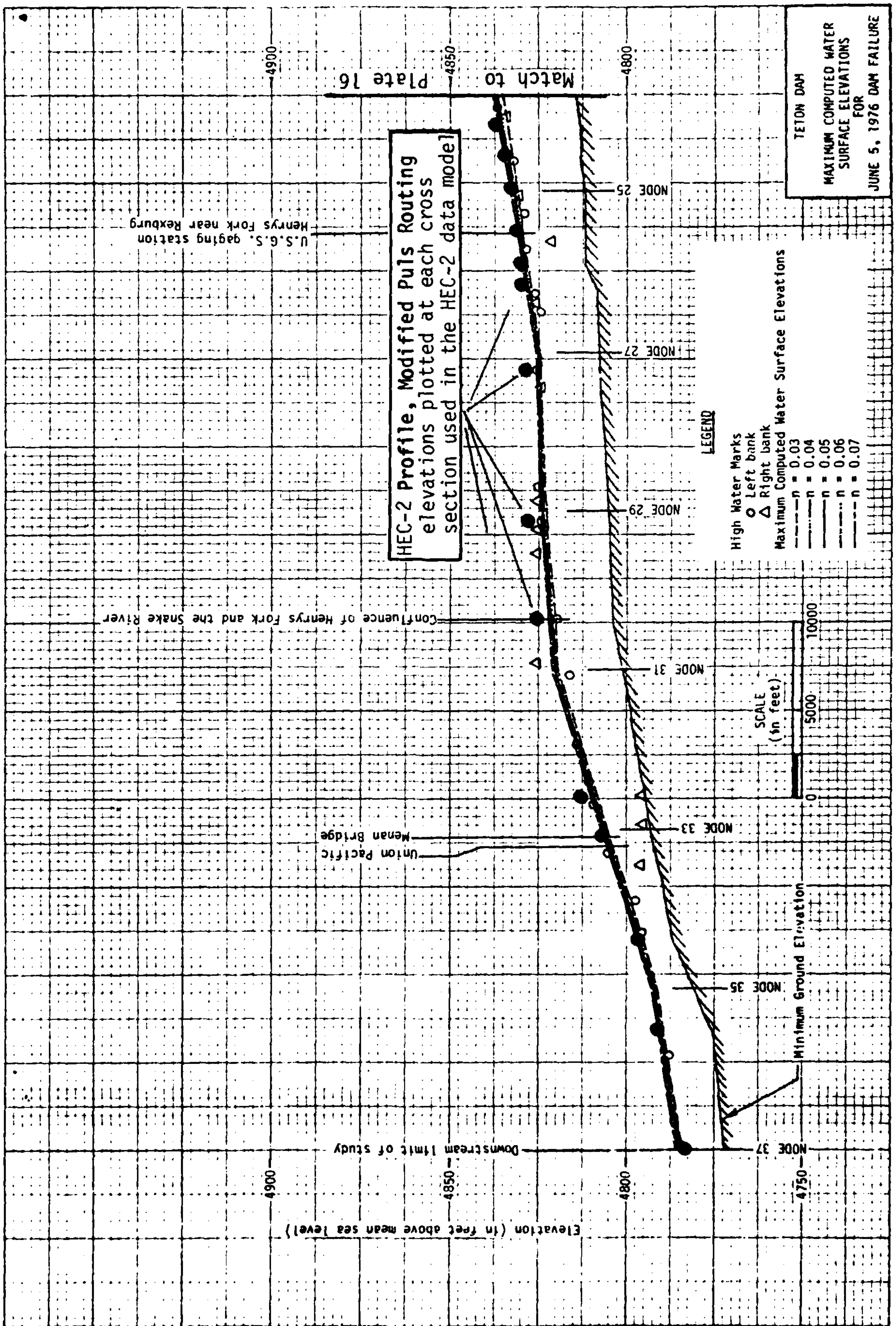

TETON DAM
MAXIMUM COMPUTED WATER SURFACE ELEVATIONS FOR JUNE 5, 1976 DAM FAILURE
Match to Plate 16
HEC-2 Profile, Modified Puls Routing elevations plotted at each cross section used in the HEC-2 data model
LEGEND
High Water Marks
o Left bank
Δ Right bank
Maximum Computed Water Surface Elevations
n = 0.03
n = 0.04
n = 0.05
n = 0.06
n = 0.07
SCALE (in feet)
0
5000
10000
NODE 25
NODE 27
NODE 29
NODE 31
NODE 33
NODE 35
NODE 37
U.S.G.S. gaging station Henrys Fork near Rexburg
Confluence of Henrys Fork and the Snake River
Union Pacific
Menan Bridge
Downstream limit of study
Minimum Ground Elevation
4900
4850
4800
4750
Elevation (in feet above mean sea level)

APPENDIX B

Guidelines for Analyzing a Dam Break Flood with the Computer Program "Gradually Varied Unsteady Flow Profiles"

1. Data Requirements

a. Topographic maps are required. The area of coverage should extend from the upper end of the reservoir in question to the most downstream point of interest. The contour interval should be less than the level of accuracy expected from the study.

b. Aerial or ground photographs are desirable. These provide hydraulic engineers with a basis for estimating hydraulic roughness coefficients. Consequently, they are not needed for the reservoir area but for the channel and flood plain.

c. Reservoir capacity curves or tables are required and may be calculated from the topographic maps. These show the volume of water stored as reservoir depth increases.

d. Breach size and shape is required and may be estimated.

e. Reservoir level at breaching is required and may be estimated from aerial photography if reservoir records are not available.

2. Assumptions.

a. It is customary to assume that the breach is developed instantly and completely to the desired size and shape. Otherwise, several instantaneous breaches of different sizes may be postulated and the resulting floods calculated.

b. Critical depth controls at all partial breaches. In view of the values presented in Table 2, main body of this report, inertia is not a major consideration over a wide range of partial breach sizes.

c. The streambed and banks are fixed (i.e., do not erode) during the event.

d. Any bridge across the stream fails instantly upon impact of the flood wave. The resulting energy loss is negligible.

3. General Procedure. The general procedure depends somewhat upon the type of breach postulated. That is, if the entire structure is removed, the final step of the analysis will calculate the outflow hydrograph from the reservoir plus route that outflow hydrograph to all downstream points of interest in a single operation.

If only a partial breach is postulated, the outflow hydrograph is calculated first and the routing to downstream points is accomplished in a separate operation. The same analytic technique is used for both.

The obvious advantage of the first approach is a savings in the time required for performing the analysis. A more significant advantage is that the method includes any submergence effects due to the rise in tailwater elevation at the dam. This submergence effect can be sufficiently large to change the shape of the outflow hydrograph from the reservoir.

Partial breaches cannot be analyzed using the first approach because the existing computer program will not accommodate a hydraulic jump. On the other hand, the rise in tailwater elevation is usually small enough so that no submergence effect develops. Therefore, the second approach is adequate.

4. Calculation of Outflow Hydrograph Using the Partial Breach Approach. The details which follow present the partial breach approach. The first step in the calculation will determine the outflow hydrograph, paragraphs a-f. Routing the flood hydrograph to downstream points is presented in paragraph 8.

a. Calibration of Cross Sectional Data to Reservoir Volume. Locate cross sections on the topographic map so reservoir volume may be calculated using the average end area technique. Include all major tributary arms in the reservoir. Code this data for the computer program "Geometric Elements from Cross Section Co-ordinates" (GEDA) and calculate the reservoir volume for the range of elevations up to full pool. This result should agree with the reservoir capacity curve. If it differs, (± 5%), cross sections which are more representative should be developed. Usually, this means recoding some of the tributary arms.

b. Geometric Model for Reservoir. Select a distance between computation nodes that complies with criteria in the routing program, "Gradually Varied Unsteady Flow Profiles" (USTFLO). Values typically range between ¼ mile (400 m) and 5 miles (15,000 m). Execute GEDA to produce the required tables of geometric properties and n-values at each computation node. The most downstream section should be at the dam axis and include the breach that was postulated.

c. Downstream Boundary. Calculate a critical depth rating curve for the breach size and shape postulated. Each elevation selected will establish an area and top width for use in the following equation.

$$Q_{cr} = A_{cr} \sqrt{g D_{cr}}$$

where:

A_{cr} = cross sectional area, square feet

D_{cr} = A_{cr}/B_{cr}

B_{cr} = top width, feet

g = acceleration of gravity feet/second/second

d. Initial Conditions. Establish the initial water surface elevation and discharge at each computation node in the reservoir. It is expedient to always select a horizontal water surface and zero discharge. Although, one may postulate whatever conditions he desires by starting the computer model at the above conditions and simulating inflow/outflow records up to the time when breaching is anticipated.

e. Upstream Boundary. Usually, the initial reservoir inflow is assumed to be zero. It may be otherwise if so desired. In either case, code the inflow hydrograph as described in the USTFLO users manual.

f. Calculating the Outflow Hydrograph. Select an interval between printouts that is very short (a minute or less) during the early part of the hydrograph (5 minutes or so). Usually, the calculated peak will occur during this interval and the time between printouts may be increased to 10 or 15 minutes. In any case, obtain a sufficient amount of printout to define the entire outflow hydrograph shape.

5. Routing the Dam Break Flood

a. Geometric Model for Routing Downstream. Locate cross sections to the downstream points of interest using information gained from the reservoir model and following steps in the users manual. Select the distance between computation nodes. (This distance does not have to be the same as that used in the reservoir when routing with a two step process. However, use the same general guidelines.) Code the data and execute GEDA to produce the required geometric data tables.

b. Downstream Boundary. If possible, set the downstream boundary a couple of nodes beyond the point of interest. Calculate a rating curve by slope-area or by extrapolating from observed values.

c. Upstream Boundary. The outflow hydrograph calculated in paragraph 4 becomes the upstream boundary for this step.

d. Initial Conditions. Establish initial conditions by calculating a base flow profile. (Zero or negative depth is not an acceptable initial condition.) It is expedient to prescribe a bank full water discharge, to let the computer model stabilize by simulating the steady flow profile for that discharge and finally to decrease the inflow, gradually, until the desired base flow discharge is reached. Simulate the base flow conditions for a sufficiently long period of time to establish a steady flow profile. Code this profile (water surface elevation, discharge) to form the initial conditions for routing the dam break flood.

e. Routing the Flood. The computer program referenced in subparagraph 1c produces both a discharge hydrograph and a water surface elevation hydrograph at every computation node. A summary table gives maximum and minimum values for elevation, discharge and velocity.

List of Research Notes

1. Research Note No. 1. A Cumulus Convection Model Applied to Thunderstorm Rainfall in Arid Regions by D. L. Morgan, The Hydrologic Engineering Center, Davis, California, December 1970.

2. Research Note No. 2. An Investigation of the Determinants of Reservoir Recreation Use and Demand: The Effect of Water Surface Elevation by William D. Carson, Jr., The Hydrologic Engineering Center, Davis, California, November 1972.

3. Research Note No. 4. An Assessment of Remote Sensing Applications in Hydrologic Engineering by Robert H. Burgy and V. Ralph Algazi, The Hydrologic Engineering Center, Davis, California, September 1974.

4. Research Note No. 5. Guidelines for Calculating and Routing a Dam-Break Flood by David L. Gundlach and William A. Thomas, The Hydrologic Engineering Center, Davis, California, January 1977.